.2

QC
879.5
.U45
no.44

U.S. National Environmental Satellite Center, Washington, D.C.
Report no.44. Processing and display experiments using digitized ATS-1 Spin Scan Camera data, by M.B. Whitney.

145 627

U.S. DEPARTMENT OF COMMERCE
NATIONAL OCEANIC AND ATMOSPHERIC ADMINISTRATION
NOAA

Technical Report

NATIONAL ENVIRONMENTAL SATELLITE CENTER NESC-44

Processing and Display Experiments Using Digitized ATS-1 Spin Scan Camera Data

WASHINGTON, D.C.
April 1968

NATIONAL ENVIRONMENTAL SATELLITE CENTER TECHNICAL REPORT

The National Environmental Satellite Center is responsible for the establishment and operation of the National Operational Meteorological Satellite System and the environmental satellite systems of the Environmental Science Services Administration. The three principal offices of NESC are Operations, System Engineering, and Research. The NESC Technical Report series is used by these offices to facilitate early distribution of research results, data handling procedures, systems analyses, and other information of interest to other ESSA organizations. Publication of a report in the NESC Technical Report Series will not preclude later publication in an expanded or modified form in scientific journals, etc. References to a paper in this series should identify it as an ESSA - NESC Technical Report.

The NESC Technical Report series in a continuation of the U.S. Weather Bureau Meteorological Satellite Laboratory Report series. The numbering follows sequentially from the MSL Report series which ended with MSL Report No. 37.

The NESC Technical Reports and the earlier MSL Reports are available through the Clearinghouse for Federal Scientific and Technical InformationU.S. Department of Commerce, Sills Building, Port Royal Road, Springfield, Virginia, 22151. Cost per item is uniform: $3.00 for hard copy $0.65 for microfiche.

Number

* 1. Cloud Conference Summary, L. F. Whitney, Jr., (July 1960) PB 163727
* 2. Analysis of Project Hugo Test Firing, December 5, 1958, L. F. Hubert, (August 1960) PB 163728
* 3. Preliminary Studies of Atmospheric Energy Parameters, J. S. Winston, (January 1961) PB 163729
4. Open
5. TIROS I - Camera Attitude Data, Analysis of Location Errors, and Derivation of Correction for Calibration, L. F. Hubert, (April 1961) N 6211116
• Supplement to 5: Canadian Grids for TIROS I, Additional Orientation Data, Errata, L. F. Hubert, (June 1961) N 6211117
* 6. Nimbus Data Utilization Plan, (Anon), (April 1961) PB 163732
7. Identification of Cloud Forms from TIROS I Pictures, C. O. Erickson and L. F. Hubert, (June 1961) N 6214286
• 8. Ice Photography from the Meteorological Satellites TIROS I and TIROS II, D. Q. Wark and R. W. Popham, (March 1962) PB 163734
* 9. Documentation for TIROS III Television Data, L. F. Hubert, (March 1962) PB 163735
*10. Infrared Flux and Surface Temperature Determinations from TIROS Radiometer Measurements, D. Q. Wark, G. Yamamoto, and J. H. Lienesch, (August 1962) N 6311881
• Supplement to 10: (April 1963) PB 165208
*11. Perspective Locator Grids for TIROS Pictures, M. H. Frankel and C. L. Bristor, (October 1962) PB 163737
12. Catalog of Supplemental Meteorological Data Concurrent with TIROS Satellite Observations (TIROS I-V), R. L. Pyle, (August 1962) PB 163738
*13. Conference on Sferics Measurements, S. Soules (Ed.), (October 1962) PB 163739
14. A Technique for Precise Analysis for Satellite Data - Vol. 1, Photogrammetry, T. Fujita, (February 1963) PB 163740
15. Calibration of Image Distortion in TIROS Wide Angle Photography, R. C. Doolittle, (July 1963) PB 163741
16. Documentation for TIROS IV Television Data, R. L. Pyle, (May 1963) PB 163742
17. On the Use of Redundancy in the Design of Operational Satellites, S. F. Singer, (April 1963) PB 163743
*18. An Analysis of CDA Station Effectiveness in Relation to Satellite Orbit, R. L. Pyle and S. F. Singer, (July 1963) PB 163744
*19. An Investigation of Meteorological Satellite Characteristics for Continuous Earth Coverage, T. I. Gray, Jr., and S. F. Singer, (July 1963) PB 163745
20. Conference on Satellite Ice Studies, M. D. Baliles and H. Neiss, (Ed.), (June 1963) PB 163746
*21. Calculations of the Earth's Spectral Radiance for Large Zenith Angles, D. Q. Wark, J. Alishouse, and G. Yamamoto, (October 1963) PB 167176
*22. Spectral Reflectance Photography of Earth from Mercury Spacecraft MA-8, S. D. Soules, (November 1963) PB 167177
*23. The Use of Satellite Cloud Photography in Numerical Weather Prediction, M. A. Ruzecki, (December 1963) AD 423269
*24. TIROS Cloud Pattern Morphology of Some Mid-Latitude Weather Systems, H. J. Brodrick, Jr., (January 1964) AD 433485
25. Infrared Photography of the Earth from Mercury Spacecraft MA-9, S. Soules, (December 1965)

(Continued on back cover)

* Out of Print.

U.S. DEPARTMENT OF COMMERCE
C. R. Smith, Secretary
ENVIRONMENTAL SCIENCE SERVICES ADMINISTRATION
Robert M. White, Administrator
NATIONAL ENVIRONMENTAL SATELLITE CENTER
David S. Johnson, Director

ESSA TECHNICAL REPORT NESC-44

QC
879.5
.U45
no.44

Processing and Display Experiments Using Digitized ATS-1 Spin Scan Camera Data

M.B. WHITNEY, R.C. DOOLITTLE, and B. GODDARD

ATMOSPHERIC SCIENCES
LIBRARY
JUL 17 1968
E. S. S. A.
U. S. Dept. of Commerce

Washington, D.C.
U.S. NATIONAL ENVIRONMENTAL SATELLITE CENTER, REPORT NO. 44
WASHINGTON, D.C.
April 1968

145 627

National Oceanic and Atmospheric Administration
TIROS Satellites and Satellite Meteorology

ERRATA NOTICE

One or more conditions of the original document may affect the quality of the image, such as:

Discolored pages
Faded or light ink
Binding intrudes into the text

This has been a co-operative project between the NOAA Central Library and the Climate Database Modernization Program, National Climate Data Center (NCDC). To view the original document contact the NOAA Central Library in Silver Spring, MD at (301) 713-2607 x124 or Library.Reference@noaa.gov.

HOV Services
Imaging Contractor
12200 Kiln Court
Beltsville, MD 20704-1387
January 26, 2009

Blank page retained for pagination

TABLE OF CONTENTS

		Page
LIST OF FIGURES		iv
ABSTRACT		1
I.	INTRODUCTION	1
II.	INPUT DATA	1
III.	DIAGNOSTIC ACTIVITIES	4
IV.	EARTH LOCATION OF PICTURE DATA	7
V.	DISPLAY	36
VI.	SUMMARY AND CONCLUSIONS	43
ACKNOWLEDGMENTS		46
REFERENCES		47
APPENDIX 1		48
APPENDIX 2		49
APPENDIX 3		50
APPENDIX 4		51
APPENDIX 5		52
APPENDIX 6		55
APPENDIX 7		56
APPENDIX 8		58

LIST OF FIGURES

Page

Figure 1. Profiles of lines which pass through the ITC section depicted in figures 14, 15, and 16 2

Figure 2. Profiles of another portion from the same four records in figure 1 3

Figure 3. Spectral analysis of image brightness 5

Figure 4. Graphs showing variation of mid-earth sample numbers from line to line, and from picture to picture 21

Figure 5. Bar graph showing variation of digitized brightness level with sample number 24

Figure 6. Gridded ATS-1 picture (April 17, 1967: 220735Z) 27

Figure 7. Gridded ATS-1 picture (June 26, 1967: 215200Z) 28

Figure 8. Gridded ATS-1 picture (June 26, 1967: 215200Z) 29

Figure 9. Gridded ATS-1 picture (August 15, 1967: 215437Z) 30

Figure 10. ATS-1 picture taken near 7 AM local time showing sunlight terminator lines 31

Figure 11. The LK2048 produced frame 34

Figure 12. The EIS produced frame (from NASA) 35

Figure 13. Hawaiian Area.
A. LK2X2 with low enhance table 37
B. Photographically scaled map of area 37

Figure 14. ITC Area.
A. Full range table 38
B. ESSA-5 frame 38

Figure 15. ITC Area.
A. Low enhance table 39
B. Portion of EIS frame, for same area 39

Figure 16. ITC Area.
A. Mid enhance table 40
B. High enhance table 40

Figure 17. Baja California Area.
A. Low enhance table 41
B. Portion of EIS frame for same area 41

LIST OF FIGURES (CONTINUED)

Page

Figure 18. Baja California Area.
A. Horizon table. Insert section using mid enhance table 42
B. ESSA-5 frame 42

PROCESSING AND DISPLAY EXPERIMENTS USING DIGITIZED ATS1 SPIN SCAN CAMERA DATA

Merle B. Whitney, Russell C. Doolittle, and Brent Goddard
National Environmental Satellite Center

ABSTRACT

Several experiments with digitally processed ATS1 Spin Scan Cloud Camera data are described. Digital pictures are presented with their analogue equivalents. Some work on earth location of pictorial data and satellite attitude determination are presented. Suggestions are made for possible improvements in hardware and processing techniques.

I. INTRODUCTION

Inclusion of a digital recording system for the Spin Scan Cloud Camera (SSCC) carried on the Applications Technology Satellite, ATS1, has provided source data for a variety of automatic data processing experiments. Of particular interest within the National Environmental Satellite Center (NESC) are those experiments which provide experience and insight toward an eventual operational geostationary environmental satellite. Specifically, there are questions concerning the quality and information content of the cloud picture data stream, and the problems involved in automatic earth location of the images. Practical problems also arise in displaying large raster, high dynamic range images.

In addressing these questions, a series of data handling and diagnostic programming activities are described in the first portion of this report. Some indications and conclusions are given. Attitude and earth locator studies are next discussed, followed by a description of available display equipment with indications of future requirements.

II. INPUT DATA

The ground station facilities including the digitizing equipment are described in a volume concerning the ATS1 satellite and spin scan cloud

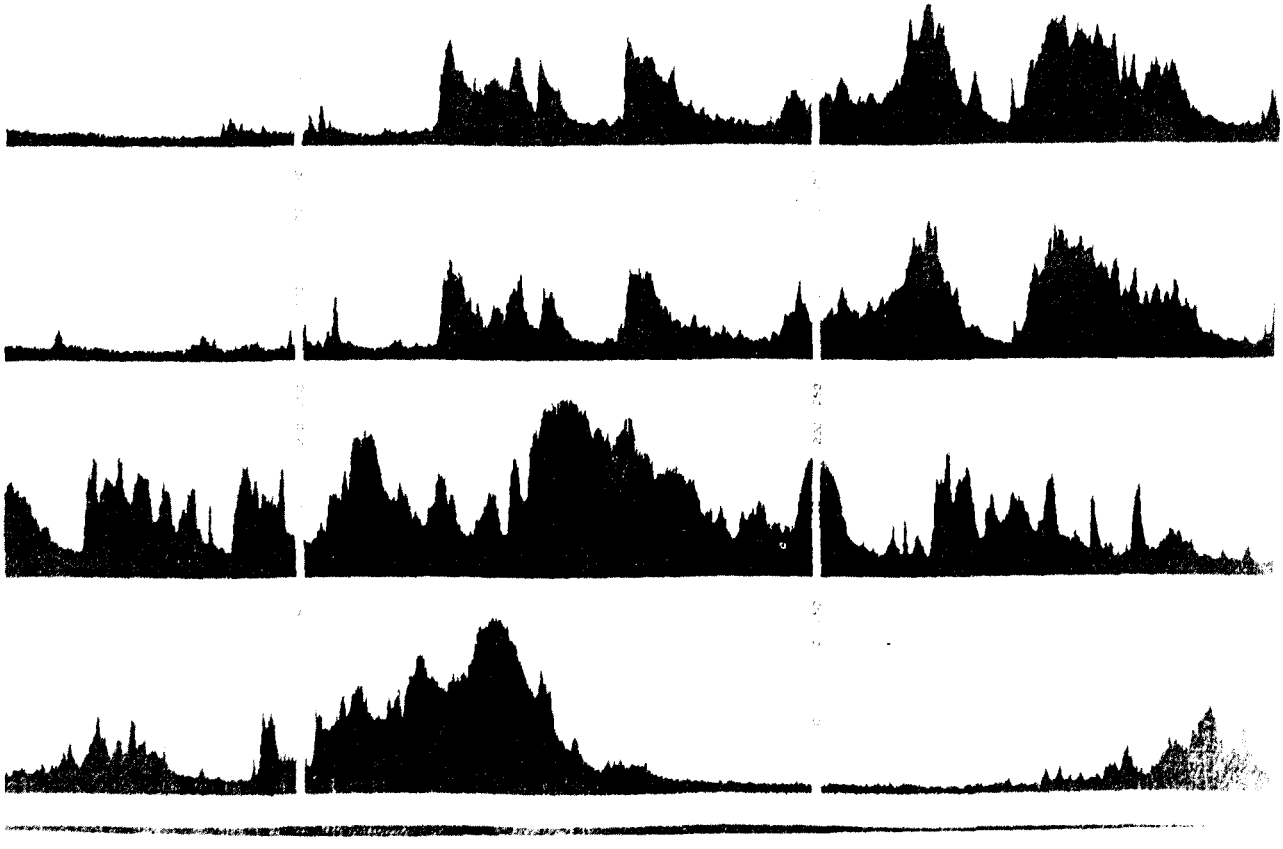

Figure 1. Profiles of lines which pass through the ITC section depicted in Figures 14, 15, and 16. The upper two profiles (records 980 and 981) are adjacent lines through the lower middle of the section. The lower middle profile (record 890) passes through the middle bright mass, the bottom profile (record 790) is through the bright mass at the top of the section.

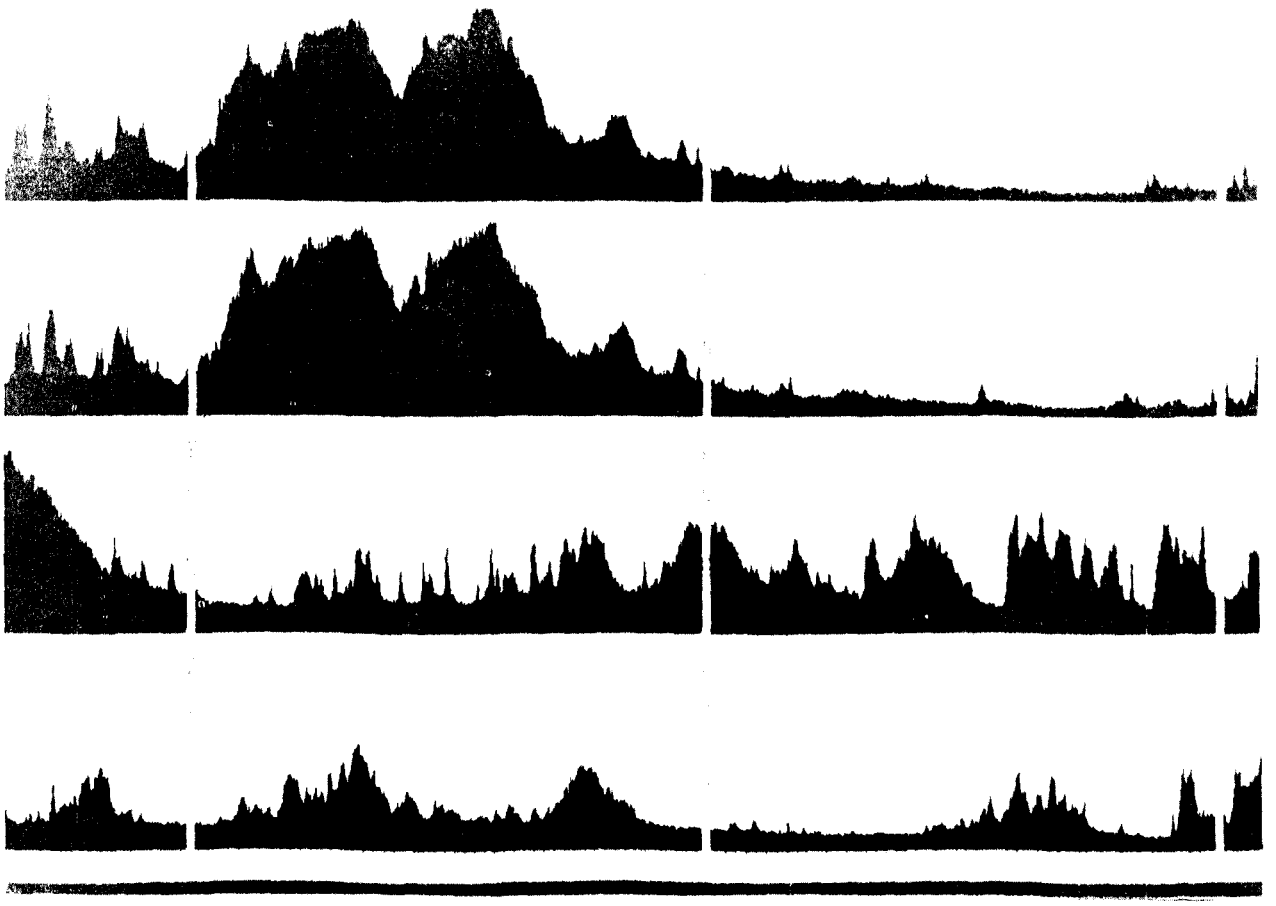

Figure 2. Profiles of another portion from the same four records in Figure 1 which also pass through a very bright mass in the center of Figure 11.

camera to be published by the University of Wisconsin Press.[1] The details of the magnetic tape format used in producing the "raw" digitized picture data are also given. Since these tapes are shared by a number of experimenters at the University of Wisconsin, NASA, etc., selected tapes are copied for retention at NESC. During the copying process, certain format changes are made and some of the space viewing response is discarded. These changes permit the compression of the raw digital data from an extended length tape to a standard 2400-foot tape. Procedures and problems involving this copy and edit program are described in Appendix 1 along with format specifications of the edited magnetic tapes.

The volume of the digital input data should be emphasized. More than 8000 partially overlapped brightness samples are obtained along each scan line and each picture contains about 2000 lines. Since each response is expressed as an 8-bit byte (0-255 count range), the total volume of digital information in a picture exceeds 128 million bits. This means that the digital information for each picture takes up an entire reel of computer tape. With the capability of producing almost three pictures per hour, the spin scan camera can provide an overwhelming volume of data.

III. DIAGNOSTIC ACTIVITIES

Since the video data volume is very large, a question could be raised as to the information content of the overlapped samples and the 0-255 brightness count range. A graphic display of the raw data values provides a qualitative answer to the question. Such profiles are shown in Figures 1 and 2. These were produced on an Alden Helix Recorder. All the data samples are displayed in full dynamic range. Close inspection of portions of the profile reveals impressive sample to sample variability suggesting large contributions to the image information content from the non-redundant portions of the overlapped samples. Broad scale continuity of the brightness masses is maintained from line to line. Large differences in the small scale features from contiguous lines indicate the absence of overlap between successive scan lines. The ability of the sensor to utilize the full 0 to 255 count range is also indicated by the profiles, thus confirming the need for the 8-bit sample.

Preferred levels in brightness profiles produced from early pictures suggested possible analog-to-digital converter problems. This prompted the adaptation of a program created for the diagnosis of similar problems involving digitized vidicon camera imagery from the ESSA satellites (see Bristor, 1966). The routine printer output from this program provides number of samples and percent occurrence information in summary form for each digital

---

[1] This volume, edited by Verner Suomi and Kirby Hansen, is now in preparation.

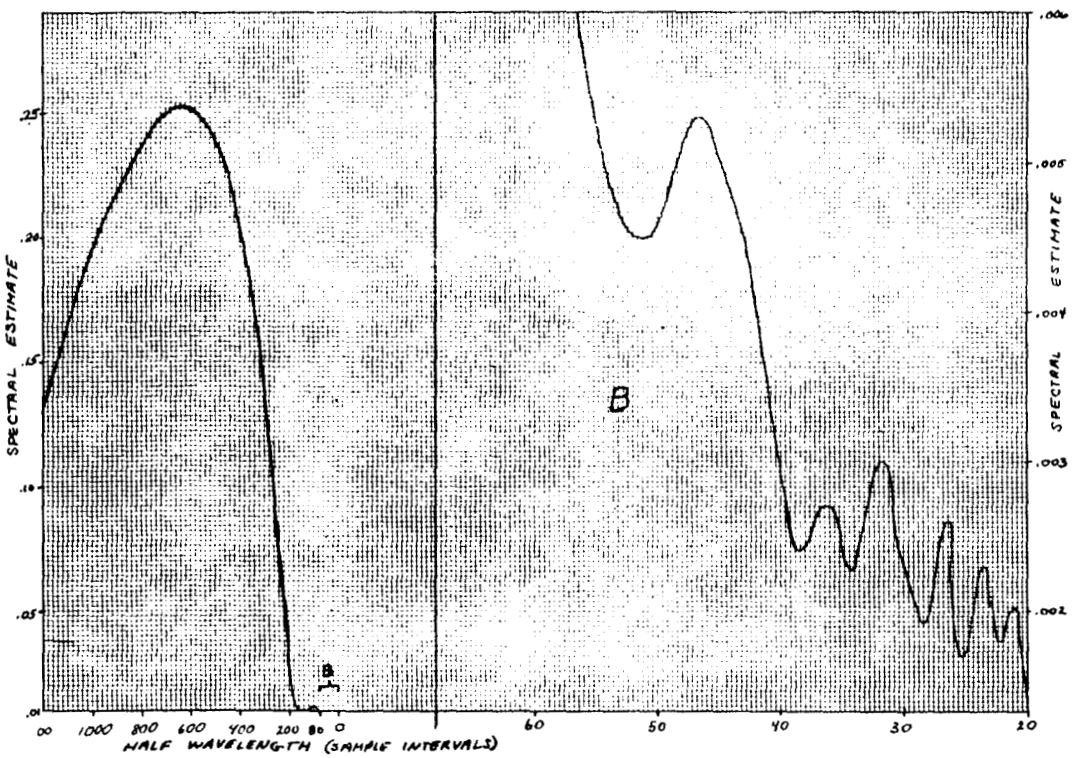

Figure 3. Spectral analysis of image brightness

brightness level. Because of its usefulness as a preliminary indicator of data quality and external problems, it was made a part of the copy-and-edit program. Beyond analog-to-digital converter problems, this routine (and the graphic profile program) has assisted in the detection of cable connector problems (evidenced as a "sticky" 8-level bit) and in problems of adjustment of the digital brightness count range.

Since the analog-to-digital converter appears over-sensitive when sequential conversions cross a binary "discontinuity" (e.g. the binary count changes from 01111 to 10000), the above program has also been amended to provide histogram information concerning the differences in sample counts between adjacent brightnesses. Plots of such summary information produce sharp peaks at the binary difference intervals (4, 8, 12, 16, 20, etc.) when such difficulties occur.

Problems with line count documentation suggest the possibility of omitted or doubled ratchets in the spin scan stepping mechanism. Toward diagnosis of such events, a program produces line summary information involving absolute brightness differences between adjacent sample pairs. Discontinuities in plots from this program have, thus far, not proven any ratcheting problem since signal imperfections at the tape writing station and/or tape read errors (computer or tape quality problems) offer alternate explanations.

Another diagnostic program computes the average brightness response for each scan line (or specified sample subset). Line-to-line plots of this quantity may help in the ratcheting question. Thus far it has provided profiles resulting from a "cross-talk" noise signal. Using space viewing raster lines accompanying an experimental moon picture, a ragged but highly repetitive 20-line noise signal (peak to peak) is very apparent. (This signal is understood to be related to the VHF experiment.)

The great variety of interesting brightness profiles displayed by the line graphics program invites study from a spectral standpoint using statistical tools.

The data for a picture taken at 2152Z on June 26, 1967, (Figure 11), in lines 976 thru 1000 and points 1501 thru 5500, were subjected to a spectral analysis to determine along-the-line signal characteristics. The spectrum peaks at a half wavelength of about 500 spots or about 350 miles and drops smoothly off to either side. Secondary peaks are frequent at lower wavelengths but are too small to interpret validly. That these do occur, however, strongly implies the existance of information thruout the spectrum. No strong indication of large amplitude noise is noticable. Figure 3 shows the plot.

IV. EARTH LOCATION OF PICTURE DATA

Geographic location of digitized image brightness from the spin scan cloud camera is required as an aid to the meteorological interpretation of the data. The digital computer programming effort described below was undertaken to provide both latitude/longitude grids to fit displayed pictures, and inputs to mapping codes which rectify the imagery to either Mercator or polar stereographic projections.

Gridding and mapping programs already in use at NESC are keyed to the geometry of the conventional perspective view and the present effort was limited to revisions and additions necessary to adapt them for use with the spin scan camera. For either gridding or mapping, the input information necessary to relate ground points on the earth's surfaces with points on an image plane includes:

1. The camera (satellite) location.

2. The three-dimensional orientation of camera coordinate axes with geocentric earth coordinate axes.

3. The location of the perspective center of the camera with respect to the image plane.

4. A knowledge of image distortion (departure of the position of imaged points from that in a true perspective geometry).

In gridding, rays from selected latitude/longitude intersections to the satellite are projected to the image plane and distortion is then applied to make the grid fit the picture. In mapping, image positions are corrected for distortion, and the perspective rays defined by the revised image coordinates are then projected to earth, and the latitude and longitude (and map position) of the intersection are computed.

Because of lack of experience with the spin scan camera this programming has a strong investigative slant with many diagnostic features and makes use of specialized existing computer codes. For that reason it is far from adequate for "real time" operational use, but rather indicates the feasibility of methods and provides a starting point for the further extensive work which would be required to provide satisfactory grids and maps for all pictures on a timely basis.

A. Satellite Location

Since both the gridding and mapping programs expect satellite location in the form of subsatellite point latitude/longitude and satellite height, a program was written to generate them from orbital elements (available from

NASA-GODDARD SPACE FLIGHT CENTER via teletype) and the date/time of pictures (received with the digital tapes from the ground station). Since this program used an idealized circular orbit geometry without regard to celestial mechanics, a check was made using an orbit generator based on the Brouwer method. (This program was developed for NASA by the General Electric Company and modified for in-house use at NESC.) Results agreed within 0.01 degrees in latitude, 0.11 degrees in longitude, and about 2 kilometers in height and were adequate for the present purpose. For operational use an orbit generator appropriate for the small eccentricity ATS earth-synchronous satellites may be desirable.

B. Attitude Determination

1. Method

The gridding and mapping input programs accept camera orientation information in the form of three angles — tilt of the optical axis from the vertical, azimuth of the principal plane (the vertical plane containing the optical axis), and swing (rotation of the principal line relative to x, y axes in the image plane). The principal line is the intersection of the principal plane with the image plane.

In the case of SSCC data, tilt, azimuth, and swing are computed for a hypothetical conventional camera with y axis parallel to the satellite spin axis, positive toward the northern hemisphere, x-axis horizontal, and z axis along the spin axis normal closest to the zenith (along the incident ray to the uncanted position of the camera telescope in the mid-earth portion of the scan).

The procedure follows:

a. Determine the instantaneous spin axis roll for each picture from the horizon image. (Instantaneous roll is defined as the angle between the spin axis and the horizontal, positive when the northern hemisphere end of the spin axis is above the horizontal.)

b. Compute the maximum displacement of the spin axis from the orbit normal, and the phase in the orbit at which this occurred, from the pattern of instantaneous roll over a picture sequence.

c. Convert the maximum roll and phase angles to spin axis right ascension and declination by rotation through the orbit inclination and right ascension of the ascending node.

d. Compute spin axis azimuth and elevation angles at each camera position.

e. Compute the orientation matrix relating local topocentric axes (east, north, up) to the camera axes by applying successive rotations in azimuth and elevation.

f. Compute tilt, swing, and azimuth for each picture from elements (direction cosines) of the orientation matrices generated in step e.

Steps a. and b. make use (with slight modification) of a method for determining spin axis attitude from horizon data taken by infrared scanners on TIROS IX and TOS "wheel" type meteorological satellites.[1]

In step a. of the procedure, the instantaneous roll ϕ_k for each picture is obtained from a least-squares solution of a system of simultaneous linear equations:

$$\cos \alpha_i \cos \beta_i \cos \phi_k - \sin \alpha_i \sin \phi_k = \cos \theta_i \qquad [1]$$

where: α_i is the displacement of the telescope from its mid-position normal to the spin axis, positive toward the northern hemisphere, for horizon point i .

β_i is the spin displacement of the telescope from the midearth point of the scan.

θ_i is the angle at the camera between the ray to a horizon point and the local vertical.

ϕ_k is the instantaneous roll of the spin axis for picture K.

The coefficients and constant terms are computed from the relationships

$$\alpha_i = (J_o - J_i) * 0.000131$$
$$\beta_i = (I_i - I_o) \times 0.00004261$$
$$\theta_i = \sin^{-1}(R/\rho)$$

where J_o is the picture line count at the undisplaced position of the telescope and J_i is the picture line count for the observed horizon point. I_i is the digital spot count to the horizon point and I_o is the spot number at the mid-earth position of the scan. R is the radius of the earth at the horizon point and ρ is the length of the

[1] "Attitude Handbook for the TIROS IX and OT-3 Meteorological Satellite System", Appendix E, prepared by Astro-Electronics Division, Radio Corporation of America for Goddard Space Flight Center, NASA, December 27, 1965.

geocentric radius vector to the satellite. (The value used for R was computed for the latitude of the mid-earth position of each scan line for a spin axis aligned with the orbit normal.) The constants 0.00131 and 0.0004261 are the angular increment in radians between successive lines (15° in 2000 lines) and successive spot numbers (20° in 8192 samples).

Finally, the instantaneous roll was computed from $\phi_k = \tan^{-1}(\sin\phi_k/\cos\phi_k)$ where the subscript K denotes position in the picture sequence.

In step b., the maximum roll and phase angles were computed from a least-squares solution to a set of linear simultaneous equations:

$$\cos W_K \left[\sin\phi_{max}\cos\lambda\right] + \sin W_K \left[\sin\phi_{max}\sin\lambda\right] = \sin\phi_K \qquad [2]$$

where W_K is the position of the satellite in the orbit, measured in radians from the ascending node.

ϕ_{max} is the maximum spin axis roll.
λ is the angular position in the orbit at which the spin axis has maximum roll.

In order to compute the coefficients ($\sin W_K$, $\cos W_K$), the orbit phase angle (W_K) was computed from the input latitude, longitude, and height.

(1) Longitude was converted to right ascension by subtracting the Greenwich hour angle of Aries at the mid-time of each picture.
(2) Geocentric Cartesian coordinates were computed for the satellite (x axis in vernal equinox, z axis along north polar axis).
(3) The corresponding direction cosines were transformed to those for a rotated coordinate system with x axis at the ascending node and y axis through maximum subpoint latitude. (ℓ, m, n)
(4) $W_K = \tan^{-1}(m/\ell)$

The system of equations [2] is solved for two unknowns:

$$A = \sin\phi_{max}\cos\lambda$$

$$B = \sin\phi_{max}\sin\lambda$$

From these, ϕ_{max} is computed as $\sin^{-1}\left(\sqrt{A^2 + B^2}\right)$ and λ as $\tan^{-1}(B/A)$.

2. Preliminary Test of Method with Ficticious Data

As a preliminary test of the method using ficticious data, a computer program was written to generate horizon spot numbers for hypothetical pictures of a spherical earth, taken from equally spaced

positions around a circular orbit. Two angles specifying the spin axis attitude were read from data cards ("Phimax" the maximum value of instantaneous spin axis roll, and "Lambda" the phase angle in the orbit at which instantaneous roll is zero and passing from negative to positive). The horizon spot numbers were generated for 21 lines at 100-line intervals on 72 pictures 20 minutes apart. Various combinations of these spot/line numbers were then used as input for determination of spin axis attitude.

When the full population of 3024 horizon points (42 points per picture, 72 pictures) was used, the computed values were correct to three decimal places for input $\phi max = 0.5^{\circ}$, $\lambda = 0^{\circ}$. For input values of ϕ max = 2°, $\lambda = 0^{\circ}$ the computed values were in error by 0.003 degrees in ϕ max and 0.001 degrees in λ. For this same input attitude, and a greatly reduced set of 38 horizon points (4 to 6 points per picture, on 7 pictures spaced around the orbit) the computed values were in error by 0.016° in ϕ max and 1.234° in λ.

3. Tests With Real Data

Attitude was determined from three sets of pictures — 4 frames taken April 17-18, 9 frames taken April 21-22, and 14 frames from August 15-16, 1967. The first covered too small a section of the orbit to give satisfactory attitude and served chiefly to point up the problems in accumulating input information. The second and third covered large portions of a day and benefitted from the experience with the earlier pictures.

a. Preparation of Inputs

The results with fictitious data indicate that satisfactory results could be obtained with a small number of horizon points (e.g. 100) which could be measured from displays of the digital data and punched into cards. However, for these tests it was more expedient to generate horizon sample spot/line numbers for each line by computer search of the digitized brightness values and input them on magnetic tape. This computer search was carried out as a secondary task in the processing of data for other purposes and could thus be done relatively inexpensively.

The search logic for computer location of the horizon sample number for each line is described in detail in Appendix 3, together with the tape format used to output the data. Because of the high data volume which had to be handled to generate these tapes, several computer runs were required to process all of the pictures in a sequence.

TABLE 1A.--Attitude computation from ATS I pictures of April 21-22, 1967

PICTURE DATE		START TIME	SATELLITE LOCATION LATITUDE	LONGITUDE	HEIGHT (KM)	ORBIT PHASE (Degrees past ascending node)
4/21/67	(1)	13:31:27	0.04N	149.94W	35791	10.10
	(2)	14:41:07	0.14N	149.95W	35792	27.55
	(3)	17:00:49	0.29N	149.96W	35792	62.56
	(4)	19:20:17	0.34N	149.97W	35791	97.51
	(5)	21:46:47	0.25N	149.98W	35788	134.23
	(6)	22:56:47	0.17N	149.98W	35786	151.78
4/22/67	(7)	01:16:12	0.02S	149.98W	35783	186.73
	(8)	03:58:57	0.24S	149.97W	35782	227.54
	(9)	06:18:28	0.33S	149.93W	35783	262.55

TABLE 1B.--Attitude computation from ATS I pictures of April 21-22, 1967--Continued

	SINE OF ROLL ANGLE	ONE SIGMA ERROR	STANDARD DEVIATION	SQUARE ROOT OF WEIGHT	RESIDUAL	SPIN AXIS ROLL (Degrees)		SPIN AXIS ERROR (DEGREES)
(1)	0.023157	±0.000012	0.000038	7.443	0.00787	1.33	(1.39)	-0.06
(2)	0.050452	±0.000414	0.000945	0.218	-0.00640	2.89	(1.21)	+1.68
(3)	0.010911	±0.000106	0.000195	0.848	-0.00123	0.62	(0.54)	+0.08
(4)	0.010463	±0.000145	0.000363	0.623	-0.01006	0.60	(-0.33)	+0.93
(5)	-0.019542	±0.000018	0.000047	4.944	0.00160	-1.12	(-1.10)	-0.02
(6)	-0.023459	±0.000009	0.000027	9.514	0.00234	-1.34	(-1.32)	-0.02
(7)	-0.028447	±0.000039	0.000105	2.305	0.00895	-1.61	(-1.39)	-0.22
(8)	-0.015180	±0.000007	0.000018	13.621	0.00114	-0.87	(-0.87)	0.00
(9)	-0.002964	±0.000060	0.000171	1.497	0.00321	-0.17	(-0.05)	-0.12

SPIN AXIS ATTITUDE

Departure from orbit normal (degrees)	1.44± .03
Position in orbit (degrees past ascending node)	354.41±1.21
Right ascension (degrees)	236.03±0.88
Declination (degrees)	88.49±0.04

TABLE 1C.--Attitude computation from ATS I pictures of April 21-22, 1967--Continued

	HORIZON DATA POINTS				NADIR POINT			PICTURE CENTER	
	NUMBER OF LINES	NOT FOUND	REJECTED	USED	SPOT	LINE		SPOT	LINE
(1)	1964	86	93	1785	3924	1133	(1177)	3923	956
(2)	1625	76	167	1382	(4945)	930	(1313)	(3833)	617
(3)	1572	50	219	1303	(5005)	744	(1180)	(3833)	564
(4)	1800	63	116	1621	(4401)	882	(1065)	(3833)	817
(5)	1479	112	269	2577	3853	322	(851)	3854	471
(6)	1917	77	94	1746	3834	766	(820)	3824	946
(7)	1783	29	33	1721	3729	628	(786)	3760	842
(8)	1800	18	59	1723	3831	849	(884)	3831	965
(9)	1800	25	6	1769	3624	898	(977)	(3833)	921

TABLE 2A.--Attitude computation for August 15-16, 1967

PICTURE DATE		START TIME	SATELLITE LOCATION LATITUDE	LONGITUDE	HEIGHT (KM)	ORBIT PHASE (Degrees past ascending node)
8/15/67	(1)	13:17:30	0.09N	149.95W	35793	60.04
	(2)	14:07:31	0.10N	149.96W	35793	72.57
	(3)	14:54:41	0.11N	149.96W	35793	84.39
	(4)	15:41:57	0.11N	149.97W	35792	96.23
	(5)	16:29:07	0.11N	149.97W	35792	108.06
	(6)	17:16:22	0.10N	149.97W	35790	119.90
	(7)	19:38:01	0.05N	149.98W	35786	155.40
	(8)	20:25:11	0.03N	149.98W	35784	167.22
	(9)	21:12:24	0.01N	149.98W	35783	179.06
	(10)	21:54:37	0.01S	149.98W	35781	189.64
	(11)	22:46:50	0.04S	149.98W	35779	202.73
8/16/67	(12)	01:55:40	0.10S	149.96W	35777	250.09
	(13)	02:42:50	0.11S	149.92W	35777	261.95
	(14)	06:38:56	0.07S	149.91W	35782	321.15

TABLE 2B.--Attitude computation for August 15-16, 1967--Continued

	SINE OF ROLL ANGLE	ONE SIGMA ERROR	STANDARD DEVIATION	SQUARE ROOT OF WEIGHT	RESIDUAL	SPIN AXIS ROLL (Degrees)		ERROR (Degrees)
(1)	0.010258	0.000052	0.000047	2.564	-0.00243	0.59	(0.53)	0.06
(2)	0.011299	0.000049	0.000045	2.757	-0.00261	0.65	(0.59)	0.06
(3)	0.012502	0.000044	0.000039	3.074	-0.00497	0.72	(0.62)	0.10
(4)	-0.007739	0.000786	0.000372	0.171	+0.00320	-0.44	(0.63)	-1.07
(5)	-0.002159	0.000769	0.000236	0.175	+0.00222	-0.12	(0.61)	-0.73
(6)	0.010592	0.000038	0.000085	3.502	-0.00308	0.61	(0.56)	0.05
(7)	0.005653	0.000025	0.000066	5.335	-0.00386	0.32	(0.28)	0.04
(8)	0.003884	0.000022	0.000053	6.179	-0.00661	0.22	(0.16)	0.06
(9)	0.001542	0.000023	0.000062	5.775	-0.00557	0.09	(0.03)	0.06
(10)	-0.001680	0.000030	0.000009	4.511	+0.00105	-0.08	(-0.07)	-0.01
(11)	-0.004150	0.000010	0.000010	13.987	+0.00386	-0.24	(-0.22)	-0.02
(12)	-0.010338	0.000009	0.000010	14.726	+0.00230	-0.59	(-0.58)	-0.01
(13)	-0.010436	0.000009	0.000010	14.683	-0.00549	-0.60	(-0.62)	0.02
(14)	-0.006791	0.000013	0.000010	10.483	-0.00422	-0.39	(-0.41)	0.02

SPIN AXIS ATTITUDE

Departure from orbit normal (degrees)	0.63±0.01
Position in orbit (degrees past ascending node)	92.07±1.12
Right ascension	47.80±1.34
Declination	89.48±0.01

TABLE 2C.--Attitude computation for August 15-16, 1967--Continued

	HORIZON DATA POINTS				NADIR POINT		PICTURE CENTER	
	NUMBER OF LINES	NOT FOUND	REJECTED	USED	SPOT	LINE	SPOT	LINE
(1)	1800	276	264	1260	3801	1087	3801	1009
(2)	1800	203	527	1070	3780	1094	3780	1009
(3)	1800	171	709	920	3760	1104	3760	1009
(4)	1800	105	827*	868*	(4248) 3783	(956) 1093	4189	1009
(5)	1800	141	697	962	(4730) 3760	(954) 1096	3760	1009
(6)	1800	185	419	1196	3780	1089	3767	1009
(7)	1800	203	4	1593	3793	1052	3793	1009
(8)	1800	167	1	1632	3796	1040	3829	1009
(9)	1800	187	3	1610	3809	1021	3809	1009
(10)	1800	219	1616	1765	3706	992	3821	1009
(11)	1800	44	12	1744	3709	977	3725	1009
(12)	1800	36	36	1728	3720	930	3722	1009
(13)	1800	30	126	1644	3727	929	3733	1009
(14)	1800	84	360	1356	3751	956	3752	1009

An auxiliary program was written to assemble the data from these tapes onto a single tape in proper sequence according to picture times. This program also prints out the horizon sample numbers for each line for verification. Also, for pictures of a fully illuminated earth disc (taken within 40 minutes of local noon) the difference in sample numbers between the left and right horizons and the shift of the mid-earth sample number from the center of the data format are computed and printed out for diagnostic use. In addition to the horizon data input on tape, the attitude program requires a number of other information items which are input on punched cards. These items which include picture identification and time, orbital elements, parameters defining the camera image geometry, and program option selection codes, are listed in Appendix 4.

b. Numerical Results

The results of the attitude computations for pictures from April 21/22 and August 15/16 are shown in Tables 1 and 2 respectively. There are three parts to each table. The first shows date and start time for the pictures used, and the satellite location (latitude, longitude, height), and position in the orbit, relative to the ascending node. The satellite positions were generated from orbital elements furnished by NASA using one of the in-house orbital generators referred to above and are therefore to some extent approximations, but close enough for the attitude computation.

The second part of each table shows the instantaneous roll computed for each picture together with error descriptors and the final solution obtained for the orbit. The standard deviations in the third column were obtained from the solution of the normal equations developed from the system of equations [1] , and are a measure of the average difference in the cosine of the nadir angle to the horizon as computed from the picture horizon data by the left-hand member of the equation, and from the satellite-earth geometry represented by cos θ_i.

The one sigma errors in sin ϕ shown in column 2 were obtained from the standard deviations using the reciprocals of the diagonal members of the inverted normal equation coefficient matrix as weights.

The relatively large errors for the second picture in table 1B and the fourth and fifth pictures in table 2B result from inaccurate horizon detection and/or uncertainty of the position of the picture center and are discussed in detail below.

In the least-squares solution for the spin axis attitude from the system of observation equations [2] , each equation was weighted according to the error in sin ϕ_k shown in the second column. The weights were introduced into the computation by multiplying each term of each observation equation by the square root of the weight. These values are shown in the fourth column. The low relative weights of the pictures with the larger errors is apparent. The residuals in the fifth column show the discrepancy between weighted values of sin ϕ as computed from horizon data for individual pictures (first column) and from the left hand members of the observation equations using the solution for the unknowns shown in brackets in equation [2] .

(Residual = Weight$_k$ $((\cos W_k A + \sin W_k B) - \sin \phi_k)$.)

Column 6 shows the instantaneous spin axis roll for each picture determined from horizon data (computed from sin ϕ in column 1), together with the corresponding value generated from the spin axis attitude and position in the orbit (shown in parentheses in the table). The last column shows the differences between the two sets of roll values, and is a better indicator of the correctness of results than the errors shown in the second column. The statistical errors point up roughness in the data whose effect is largely eliminated in the least-squares solution for data with normal error distribution, but do not reflect systematic bias from the correct values.

The computed solutions for the spin axis attitude are shown at the bottom of tables 1B and 2B with their one sigma errors. (The corresponding probable errors may be obtained by multiplying by 0.675.) Attitude is shown in two sets of coordinates: 1) Inclination of spin axis to orbit normal, and location relative to ascending node of plane containing orbit normal and spin axis vector; 2) Right ascension and declination of geocentric vector parallel to spin axis.

Because the orbit is so nearly equatorial, the inclination to the orbit normal is nearly equal to the codeclination. The relatively large errors in orbit location, and in right ascension, are deceptive because they occur near the polar axes of the coordinate systems where the angles are poorly defined. (Two vectors displaced in slightly different directions from alignment with the north polar axis could differ in Right Ascension by 180°.)

The values determined are the best obtained from several computer runs made for each picture sequence as improvements were made in horizon detection techniques and in methods of treating bad data input. At this writing other changes in procedure are

being tested which should improve the accuracy of roll determination in the pictures with the largest errors but results are not yet available.

c. Error Considerations

Errors in the determination of spin axis attitude from the system of equations arise principally from 1) the line (Jo) and sample (Io) numbers assigned to the picture center, 2) the sample numbers (I) found for the horizon, which determine the coefficients of the left hand member through the relationships:

$$\alpha_i = (J_o - J)\ 0.000131$$
$$\beta_i = (I - I_o) \times\ 0.00004261$$

These are discussed in detail below. The accuracy is also affected by the correctness of the numerical constants in the equations for α and β and by approximations used in the computation of cos θ. The constant 0.000131 (radians) is the incremental angle stepped for each line by the camera telescope in traversing from 7.5° above the mid-position to 7.5° below in the 2000 lines of a picture. This value was taken on faith and is not thought to have caused serious error. The constant 0.00004261 (radians) is the incremental angle between successive samples of a line as the telescope rotates about the spin axis and data from a 20-degree portion of the spin cycle is digitized into 8192 samples. Experimental check of this constant was made from horizon data and it was found to be correct within the limits of experimental error. The procedure is outlined in Appendix 5. The values obtained with their standard deviations are:

For April 21/22: 0.00004290 ± 0.00000775
For August 15/16: 0.00004225 ± 0.00000014

These two values bracket the nominal value 0.00004261 and the departures of each mean from the nominal value (0.00000029 and 0.00000036) are not significant.

The computation of cos θ involves approximations in that the nadir angle to the horizon point is computed for tangency to a sea-level spheroid using the latitude of the midearth point of the scan and neglects both the elevation of the point at the space/earth interface which forms the image horizon, and the difference in radius of the earth between the latitudes of the midearth portion of the scan and the horizon points. More accurate values of cos θ could be obtained with a procedure similar to that described in Appendix 5, by assuming the spin axis to be along the orbit normal, computing horizon spot/line numbers for each picture under that assumption, and adjusting the attitude so that the residuals between the computed and observed horizon points are minimal.

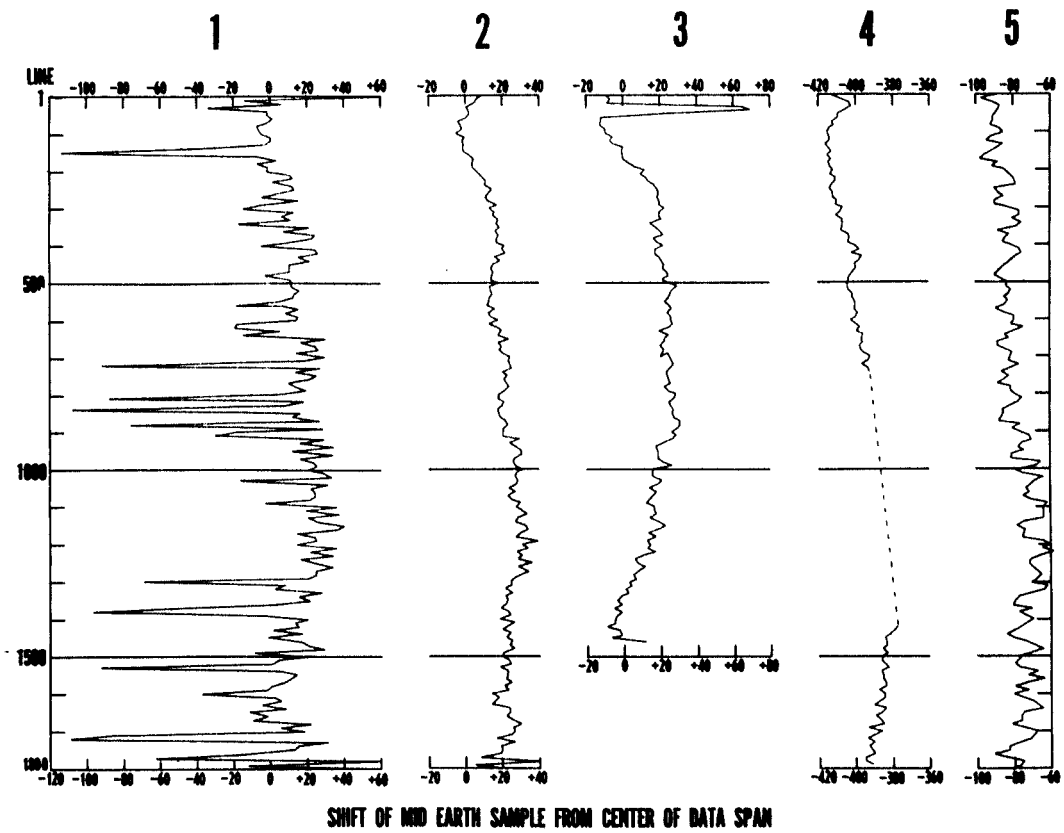

Figure 4. Graphs showing variation of mid-earth sample numbers from line to line, and from picture to picture. Horizontal scales are sample numbers with zero representing the central sample number of a line. Date/times for the pictures are: 1 and 2: 4/17/67, 220735; 3: 4/21/67, 214647; 4: 6/26/67, 215200; and 5: 8/15/67, 215437.

Time did not permit use of that approach, but in any event the errors from approximations in cos θ are small relative to those from incorrect picture center coordinates and incorrect horizon detection.

In an ideal case the mid-earth sample numbers for each line would be identical and central in the data population. (Sample number 4096 in the original data at 8192 samples per line. Sample number 3833 in the reduced population of 7665 samples formed by cropping 256 samples from each end of the original data line.) In the real data processed the midearth sample numbers depart from the ideal both in varying from line-to-line in an oscillatory curve with amplitude of 20 samples or more, and in being shifted from the middle of the data for the line. This can be seen from the graphs of Figure 4 where the mid-earth points (half way between the two horizons) are plotted against line number, for pictures taken near local noon on April 17 and 21, June 26, and August 15. The variation from line-to-line is apparent in graphs 2 and 3 and an extreme example of shift from the center is shown in graph 4 where the offset is some 400 samples so that the left horizon was never recorded in the central lines of the picture. As this displacement is more serious in magnitude than the line-to-line variation, the attitude program included a diagnostic section to compute the location of the image nadir point (earth center). The method is described in appendix 6. The picture center sample number is the same as that of the image nadir point and this permits evaluating the shift from the nominal center in pictures with only 1 horizon. The values obtained are listed in the fifth and sixth columns of Tables 1C and 2C. The values shown in parentheses for pictures 2, 3, and 4 in Table 1C and pictures 4 and 5 in Table 2C are grossly in error because of a defect in horizon detection procedure. This was corrected and the revised values for pictures 4 and 5 in Table 2C are shown below those originally obtained. (The sample numbers for the picture center in the seventh column are those input on data cards and were based on results from earlier computer runs with the same data. In some cases they are the same as for the nadir, in other cases slightly different, and where no good value for the nadir point was available, the nominal picture center 3833 was used.)

More serious than the departure of picture center sample number from nominal is the uncertainty in picture center line number when processing portions of a picture. The first column of tables 1C and 2C shows the number of lines on each picture. In table 1 the number varies markedly and in one case is 500 lines less than the 2000 odd lines of a complete picture, so that the location of the picture center is not adequately known. In the case of the fifth picture, if the 1479 lines are from the start of a picture of 2017 lines, picture center is at line 1009. If,

on the other hand, they are the last lines in the picture, the center is at line 471. The computed roll value varies significantly with the line number of the picture center. In equations [1] both coefficients of the left hand member are functions of the angle α_i, computed from $\alpha i = (Jo - Ji) * 0.000131$, where Jo is the line number of the picture center. In the above example if the center line were 1009, the sine of the roll would be -0.089 instead of -0.020 obtained using 471 for Jo, and the roll would be -5° instead of -1°.

In order to assess the potential accuracy of the attitude determination procedure when picture center coordinates are known, an attempt was made to compute them from the horizon data themselves using the iterative minimum variance techniques outlined in Appendix 7. This gave satisfactory results in some cases but failed completely in others. A simpler iterative procedure was also tried, with reasonable results for one picture, but has not been well tested. In this procedure, the spot/line numbers of the image nadir point (earth center) is computed by the method of Appendix 6. The picture center sample number is equal to that of the image nadir point, and the picture center line number is computed from:

$$Jo = J_N - \phi / 0.000131$$

Where J_N is the image nadir point line number, and ϕ is the spin axis roll angle computed in the previous iteration.

Fortunately the problem of picture center location has been solved at the readout station by digitizing only every other picture so that each tape contains a complete picture. This is reflected in Table 2C where the number of lines shown in the first column is 1800 for each picture. Actually the digital tapes received from the ground readout station for this orbit contained complete pictures. The cutoff at 1800 lines was an unnecessary (in this case) protection against running tapes off the reel. (Some earlier tapes contained data to the end of tape and did not have a terminating end of file.) Corroboration that the lines processed are the first 1800 lines of each picture is given by the orderly progression of nadir point line numbers (Table 2C, sixth column) with the variation of spin axis roll angle around the orbit. (The same orderly progression may be seen in the 6th column of Table 1C where corrected nadir point line numbers, obtained by adjusting coordinates so that the picture center would fall at line 1009, are shown in parentheses.)

In addition to incorrect sample/line numbers for the picture center, errors in the sample/line numbers of individual horizon points presented a problem. Variations in line count caused by multiple rachetting of the telescope between scans,

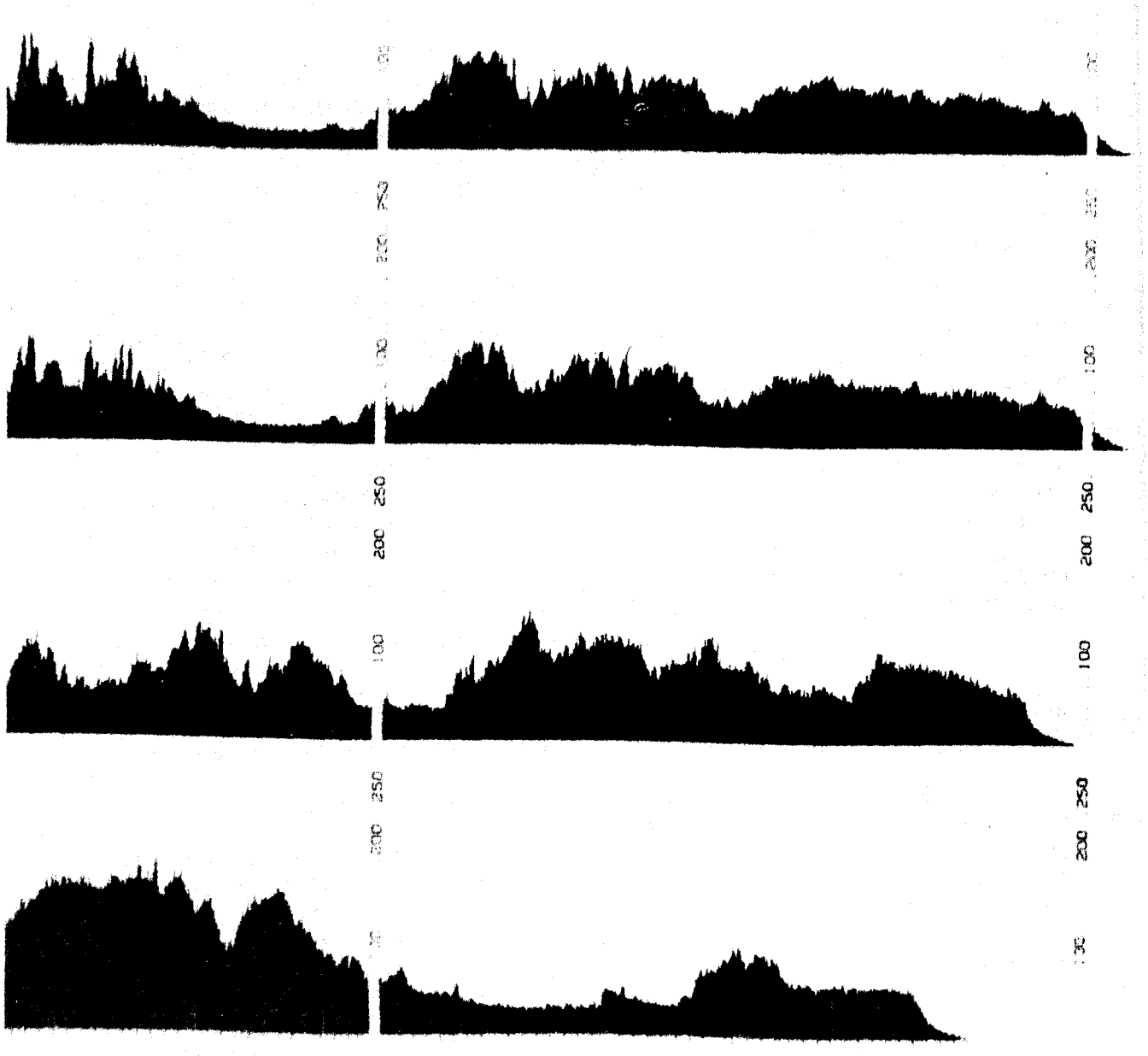

Figure 5. Bar graph showing variation of digitized brightness level with sample number, for portions of 4 lines of an ATS-1 picture which include the right horizon.

or by failure to rachet are not serious and are adequately handled by the least-squares solution. The most troublesome source of error arose from the large number of incorrect horizon sample numbers resulting from inadequacies of the computer horizon detection logic. The second, third, and fourth columns of Tables 1C and 2C show, for each picture, the number of points where the horizon was not found, the number of points rejected in the least-squares solution, and the number used. The number of bad determinations is especially large in pictures taken before noon, and is caused by low-level brightness fluctuations near the sun terminator which were falsely interpreted as earth/sky interface. This problem was solved by using separate values for the sky/earth and earth/sky thresholds for horizon detection in pictures of the "crescent earth". By using a higher sky/earth threshold to establish earth as the search procedes outward from the picture center, earth is detected closer to the illuminated horizon and the dimly lit portion near the terminator is bypassed. The improvement in horizon detection is indicated by the nadir point spot/line numbers for the fourth and fifth pictures in table 2C.

In order to filter out the large number of bad data points, a loop was added to the least-squares subroutine to analyze the frequency distribution of residuals formed from the initial solution, and where a double peaked distribution was present, to reject data from the peak with the fewest points. This worked well except for the fourth picture of Table 2C where the bad points outnumbered the good and were used in the solution. The picture was reprocessed using the improved detection technique with much better results as indicated by the improvement in computed nadir spot/line number.

The importance of adequate horizon detection techniques is illustrated in Figure 4 where graphs 1 and 2 are for the same picture. In the first graph the large scatter in the mid-horizon point data is caused by noise in the space portion of the view when an earth/sky threshold of 1/0 is used. The improvement in the second graph was obtained by setting the threshold to 6/5 in the digitized brightness scale. Because of the rapid increase of brightness at the sky/earth interface (which may be seen in the samples of Figure 5) the horizon sample number is shifted only slightly inward by use of the higher threshold. There may in fact be an additional slight increase in accuracy because the inward shift of a few samples approximates the angular difference in rays to cloud horizons, and to the earth's surface used for computing cos θ.

Spin axis attitude for the ATS-1 Satellite can be determined from Spin Scan Cloud Camera horizon data with an accuracy comparable to that obtained from the data provided by infrared

horizon detectors used in meteorological satellites. In the two determinations described here, errors were in the range of 0.01 to 0.05 degrees. This accuracy could perhaps be improved because these results include errors caused by defects in the horizon detection technique which have since been eliminated. (Some slight additional improvement could perhaps be achieved by use of iterative minimum variance techniques to improve an initial attitude estimate.)

If the data from ATS-1 is to be processed operationally, and if attitude is to be determined from horizon data, it will be important to process all of the lines of each picture (without an arbitrary cutoff at 1800 lines) because, for small departures of the spin axis from the orbit normal, the change in horizon position with spin axis attitude is most pronounced at the top and bottom of the picture.

Because of the large data volume required to obtain one attitude determination it will be advisable to integrate the various programs and to use the computer disk for temporary storage to eliminate magnetic tapes at program interfaces.

C. Picture Grids

In order to produce SSCC pictures with superimposed latitude/longitude lines, modifications were made to an existing computer program. The output of this program is a magnetic tape containing the picture spot/line numbers for points on the grid line. (This tape, together with a tape of digitized picture element brightness, provide input to a second computer code which superimposes grid lines onto the picture by altering the brightness of selected picture elements on the grid lines. This program has options to generate tapes compatible for input either to a facsimile printer, or to a LINK CRT display device operating in its digital mode.)

The required modifications were additional input information read from punched cards and revision of the subroutine which converts direction angles of incident rays from grid points on the earth to spot/line coordinates in the picture.

In addition a new subroutine was written to generate image coordinates of points on sunlight terminator lines at sea level and at other desired elevations specified on input cards. This program takes into account the shift of terminator line caused by motion of the satellite during the 20-minute duration of the picture, but does not take atmospheric refraction into account. An improved version which applies the average refraction for a standard atmosphere is in the debugging stage.

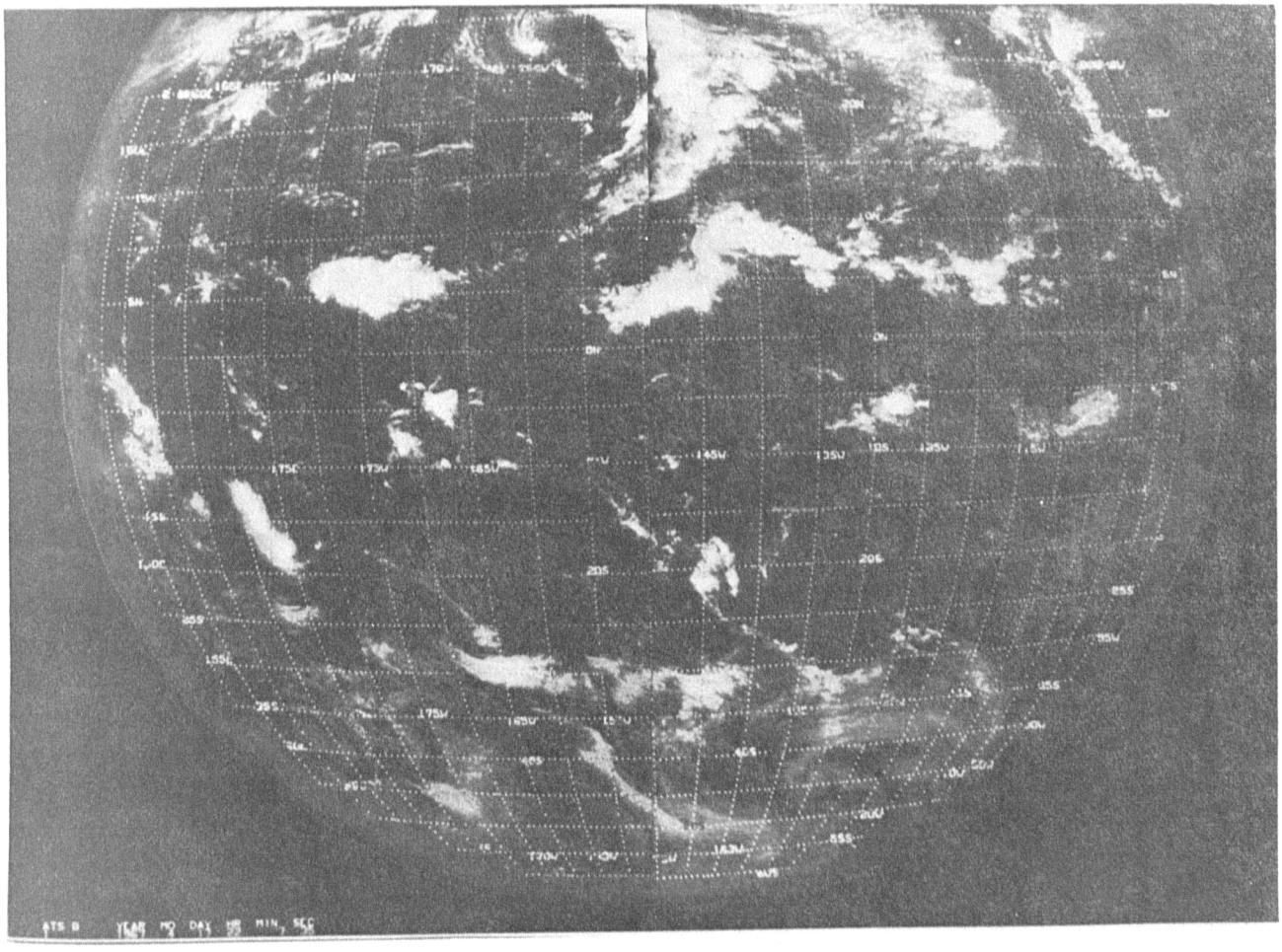

Figure 6. Gridded ATS-1 picture (April 17, 1967: 220736Z). The grid marks are obtained by a digital melding process in which the brightness value of picture elements along the grid lines are modified in the computer before the digital tape to drive the LINK CRT device is written.

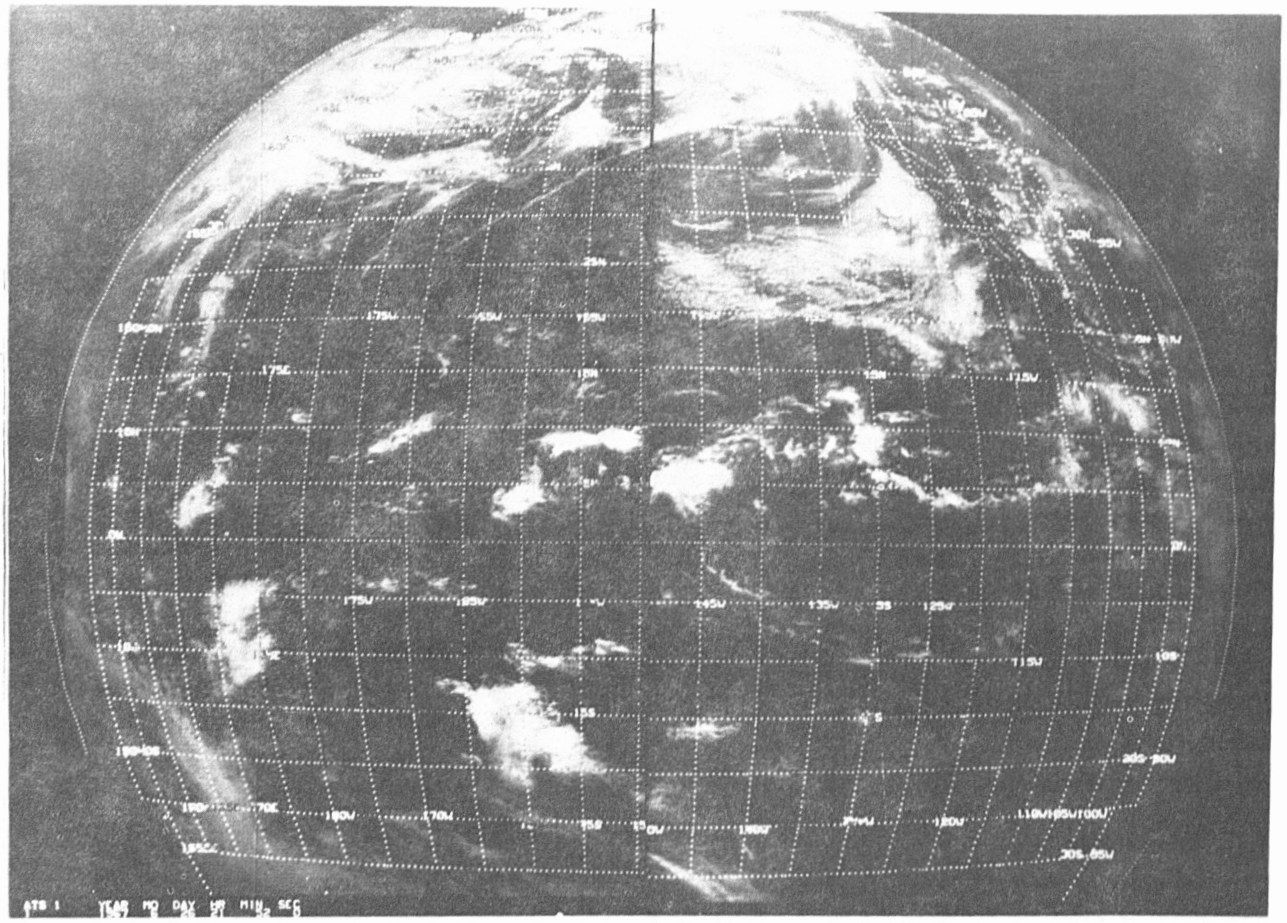

Figure 7. Gridded ATS-1 picture. (June 26, 1967: 215200Z)

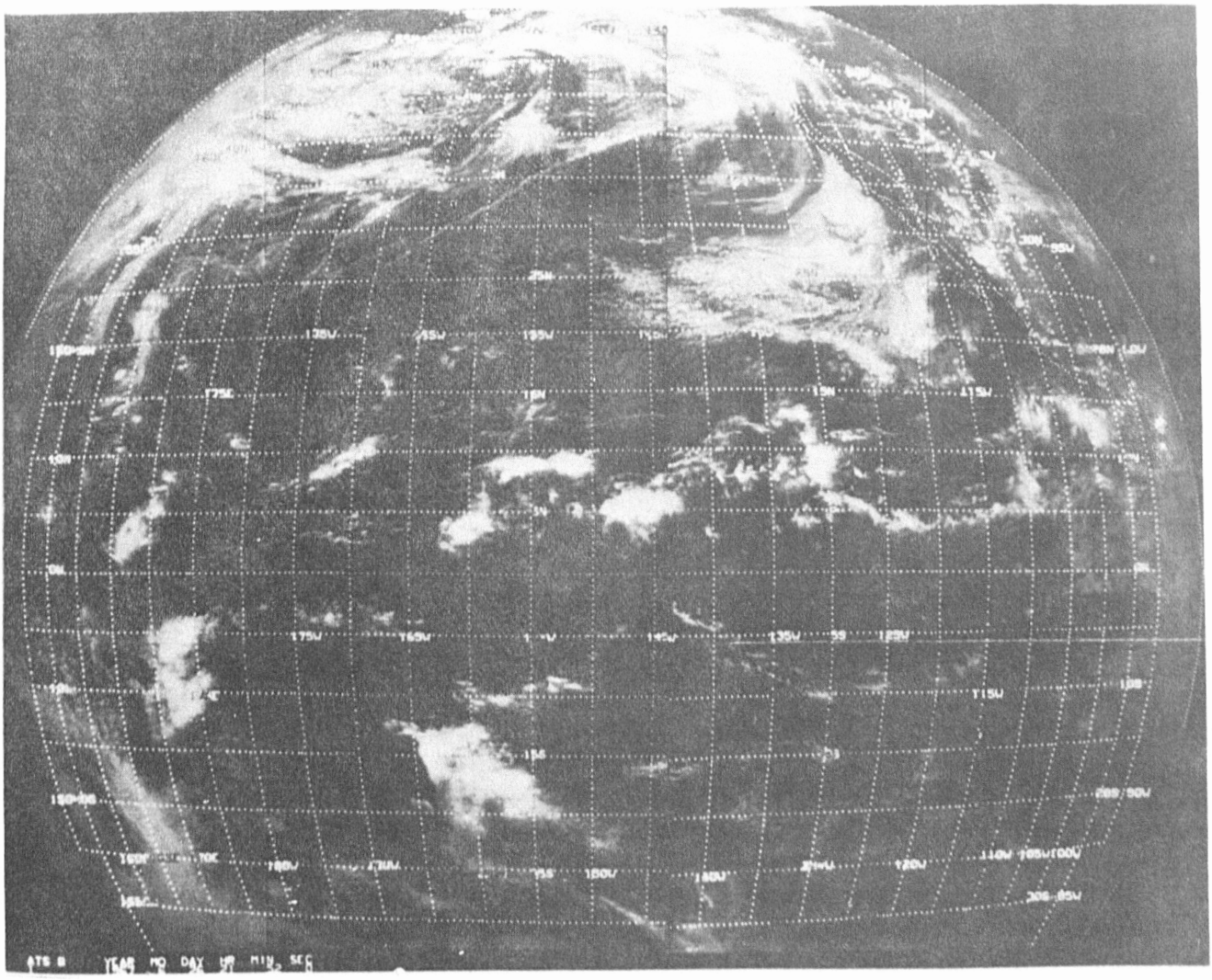

Figure 8. Gridded Picture from ATS-1. (June 26, 1967:215200Z) This is the same picture as in Figure 7 with the brightness elements of each line shifted laterally so that the mid-earth points are in a straight line from top to bottom, centered in the format.

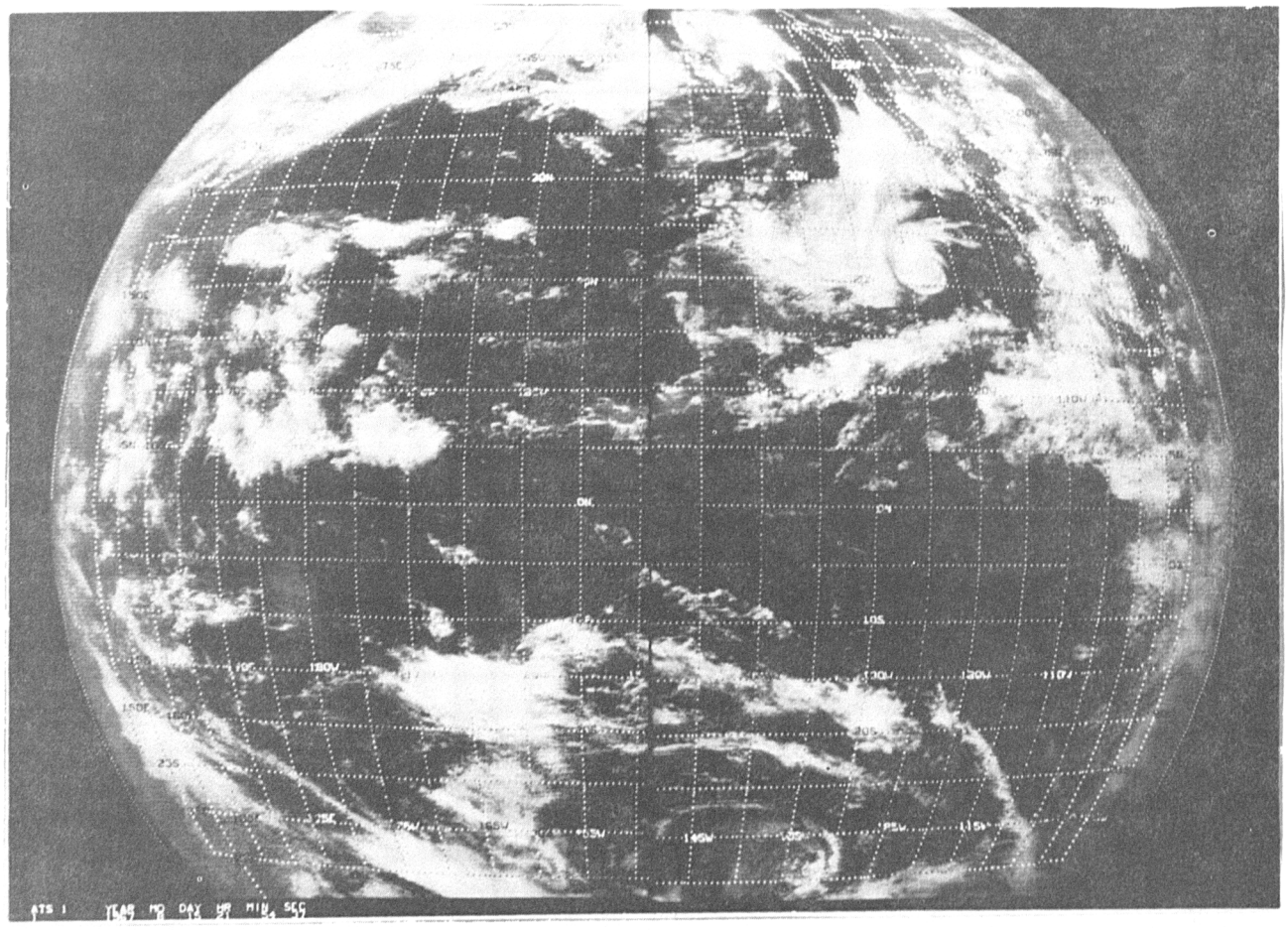

Figure 9. Gridded ATS-1 picture. (August 15, 1967: 215437Z)

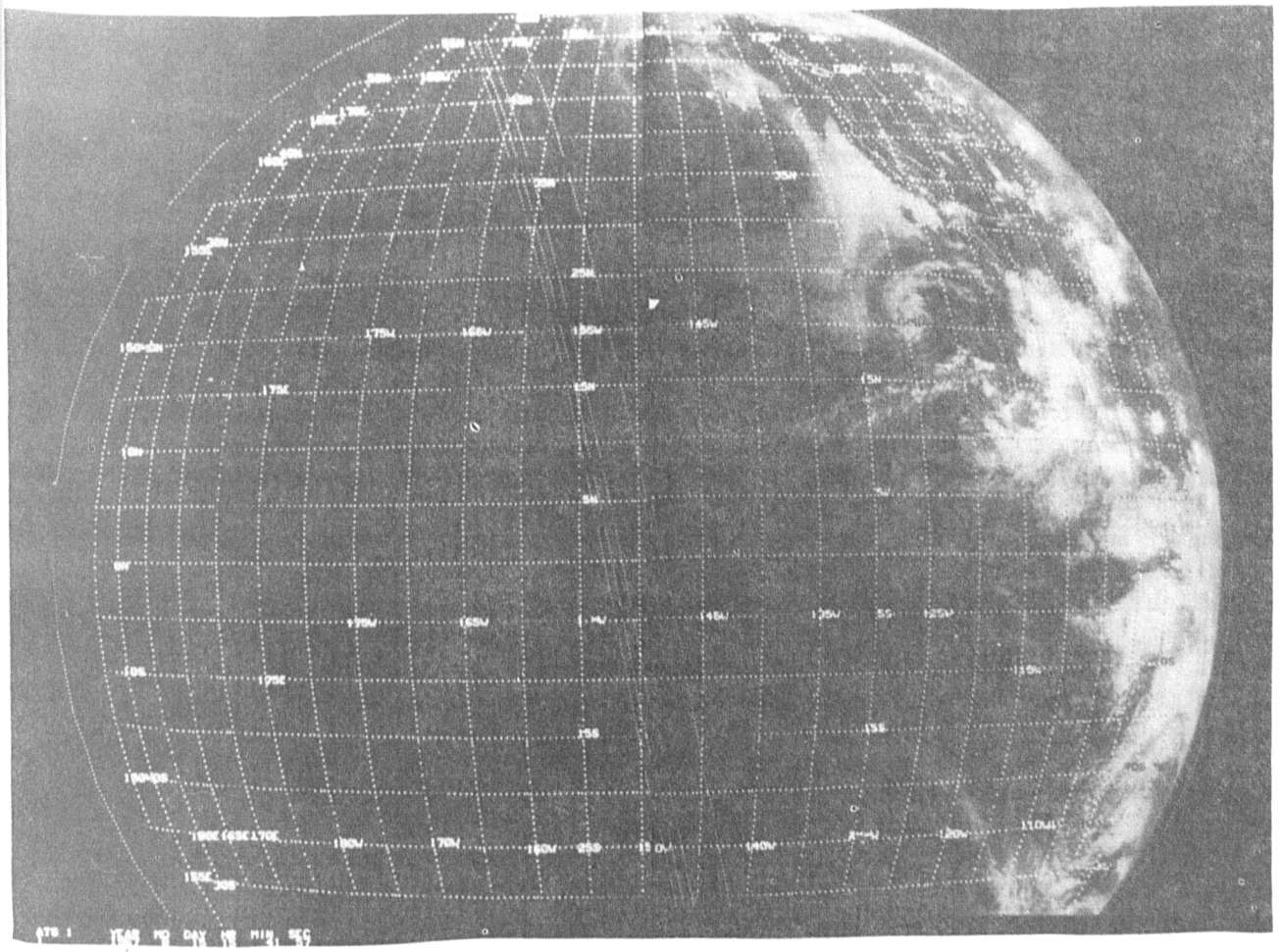

Figure 10. ATS-1 icture taken near 7 a.m. local time showing sunlight terminator lines for sea level, and for 10,000, 20,000, and 30,000 foot elevations. (August 15, 1967: 171622Z)

One unresolved problem in the gridding of the ATS data has been the technique to be used when lines are missing from the digital data. One solution involves insertion of a blank line in its proper location where there is a missing line within a picture. With the data available at this writing, there is some doubt of the line counts furnished with the digital data and there has been a failure in the hardware furnished line counts in the hundreds and thousands positions.

Examples of gridded pictures are shown in Figures 6 through 10. Figures 7 and 8 show the same picture. In Figure 7 the picture is located in the display raster with the orbital line and sample numbers of the digitized brightness elements. In Figure 8 the picture lines have been shifted in such a manner that the mid-horizon points of each line are moved to the center of the display format. This shift is done on the computer in the same program that detects horizon points and not only centers the picture in the format but corrects line-to-line offsets in the original data due to slight imperfections in the smoothed sun-pulse synchronizing circuits. Proper line-to-line synchronization is necessary for accurate gridding or mapping since both assume coherent picture geometry. Figure 10 shows a morning picture (6 AM local time) with the right horizon illuminated and sunlight terminator lines for sea level and at 10,000, 20,000 and 30,000 feet. Terminator lines may permit some approximation of cloud heights. Thus a cloud which is illuminated and located between the 10,000 and 20,000 ft. terminator lines must be at least at 10,000 feet.

In all of the gridded pictures shown, major coastlines have been added at the same time the perspective latitude/longitude grid was superimposed on the picture. This supplements the grid and also in a test phase gives another check on the accuracy of attitude and gridding programs. The techniques for use of these coastline data have been previously described (Frankel, 1962).

D. Mapping Picture Brightness

The "benchmark" program provides input to the programs which map picture brightness. For video data from "AVCS" television cameras used in meteorological satellites, coordinates of regularly spaced points in the image raster (corrected for lens and electronic distortions measured in a prelaunch distortion calibration (Doolittle, 1963)) are combined with the satellite location and the camera orientation to compute the latitude/longitude of the points, and the corresponding map coordinates on Mercator and polar stereographic projections.

The required modification for the SSCC replaces the corrected coordinates of the image benchmark points (which for AVCS pictures are read in as tables generated in the prelaunch distortion calibration) with equivalent coordinates generated point by point from sample/line numbers of the ATS pictures. The difference in image-forming geometry between the conventional pictures and those taken with the spin scan cloud camera are considered in Appendix 8.

TABLE 3.1

ATS1/LINK BRIGHTNESS TABLES

LINK	FULL RANGE	a LOW ENHANCE	c MID ENHANCE	b HIGH ENHANCE	c HORIZON
14	235 - 255	171 - 255	159 - 255	244 - 255	235 - 255 6 - 7
13	215 - 234	101 - 170	149 - 158	235 - 243	215 - 234
12	196 - 214	51 - 100	140 - 148	228 - 234	196 - 214
11	179 - 195	43 - 50	132 - 139	221 - 227	179 - 195
10	163 - 178	38 - 42	125 - 131	215 - 220	163 - 178
9	118 - 162	33 - 37	118 - 124	210 - 214	118 - 162
8	133 - 147	28 - 32	112 - 117	205 - 209	133 - 147
7	118 - 132	25 - 27	106 - 111	200 - 204	118 - 132
6	102 - 117	22 - 24	99 - 105	195 - 199	102 - 117
5	85 - 101	19 - 21	92 - 98	190 - 194	85 - 101
4	78 - 84	16 - 18	84 - 91	184 - 189	78 - 84
3	60 - 77	13 - 15	75 - 83	178 - 183	60 - 77
2	41 - 59	10 - 12	66 - 74	171 - 177	7 - 59
1	21 - 40	7 - 9	56 - 65	161 - 170	21 - 40
0	0 - 20	0 - 6	0 - 55	0 - 160	0 - 5

Figure 11. The LK2048 produced frame.

Figure 12. The EIS produced frame (from NASA).

This modification has been completed and a sample input tape for the mapping programs has been written, but at this writing has not been used with the revised mapping codes to test its correctness. Techniques of video mapping have been previously described (Bristor et al, 1966).

V. DISPLAY

At NESC we have two display devices, the FAX and the LINK, which can use digital tapes as their input source. A brief description of each is contained in Appendix 2. They are operated off line from the computer. There were 4 programs written to display pictorially the SSCC data. They all use the copy-and-edit program output as their source. To maintain the same approximate areal coverage in the E-W direction as in the N-S direction, the LK2048 program and the FAX program use every 3rd sample along the scan line to produce the image while the full resolution programs, LK1024 and LK2X2, use every data sample along the scan line and generate 2 scan lines between each pair of data lines by interpolation. The FAX program produces full disk image. The LK2048 program creates an 2048 mode image which is 80% of the full disk when every third sample is displayed. The other two programs are used to display an arbitrary section of the disk at full resolution and in 1024 mode on the LINK, The LK1024 program makes an image of 1024 adjacent samples of 330 consecutive scan lines. To experiment with digital magnification, the LK2X2 program takes each data sample and makes a 2X2 matrix of it and formats the matrices for display in the 1024 mode on the LINK. Each LK2X2 image, therefore, consists of 155 consecutive lines of 512 adjacent samples.

The large dynamic range of the sensor allowed ample opportunity to experiment with data to display conversion techniques. The lookup tables used by the programs to produce the images in the following section are given in Table 3. There was no attempt to calibrate, to apply solar illumination corrections, or account for the different possible gain settings on the satellite or ground station.

The samples of the digital data in the following set of figures are made from the picture taken on June 26 at 2152Z. All pictures were developed without the aid of a greyscale wedge on the film. The vertical dark lines are caused by display equipment problems and are not contained within the source data.

The output from LK2048 is shown in Figure 11. The full range table was used. The bright tropical clouds have been clipped at the high end at the ground station. A print, made from the second generation negative of the Electronic Image System (EIS) cathode ray tube display, was enlarged photographically to the same size as Figure 11 and is shown in Figure 12.

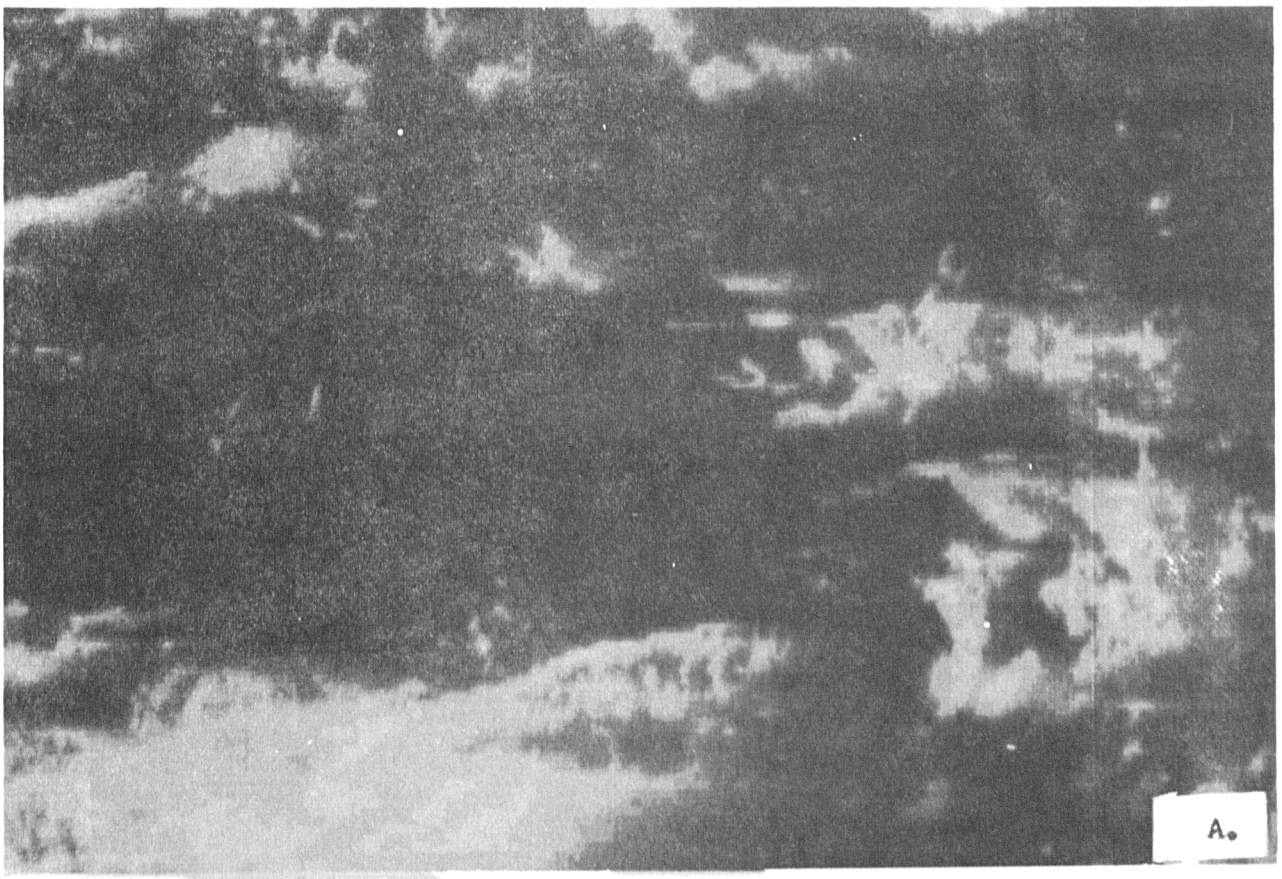

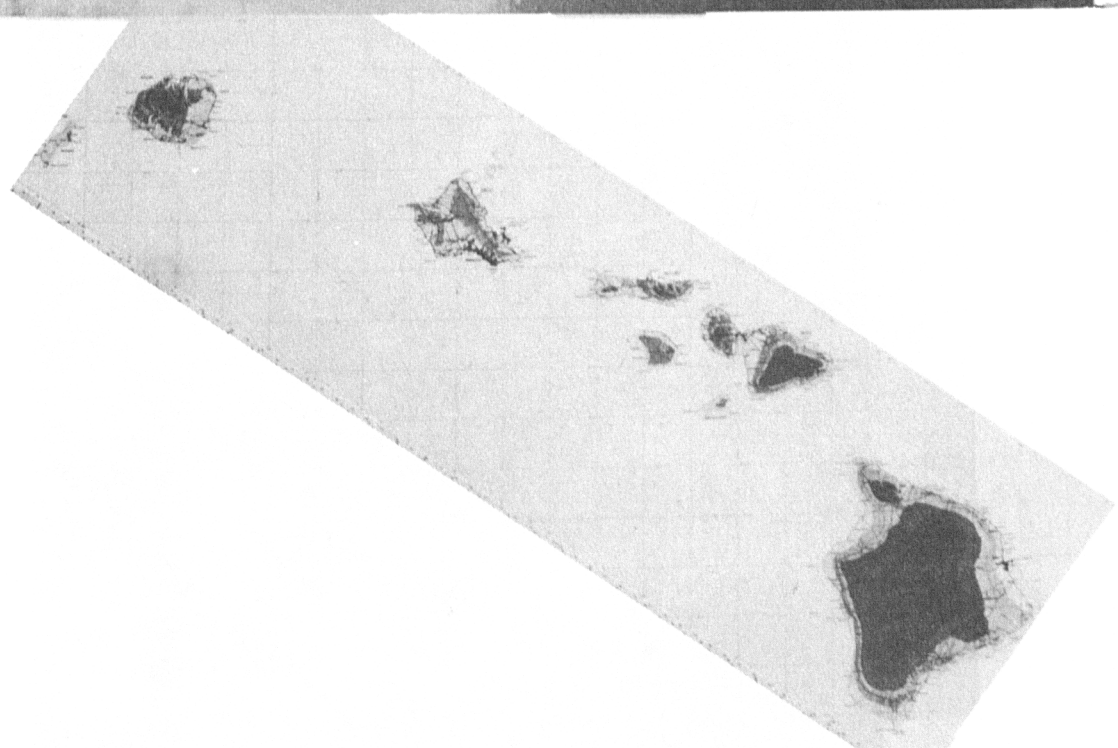

Figure 13. Hawaiian Area.
A. LK2X2 with low enhance table.
B. Photographically scaled map of area.

A.

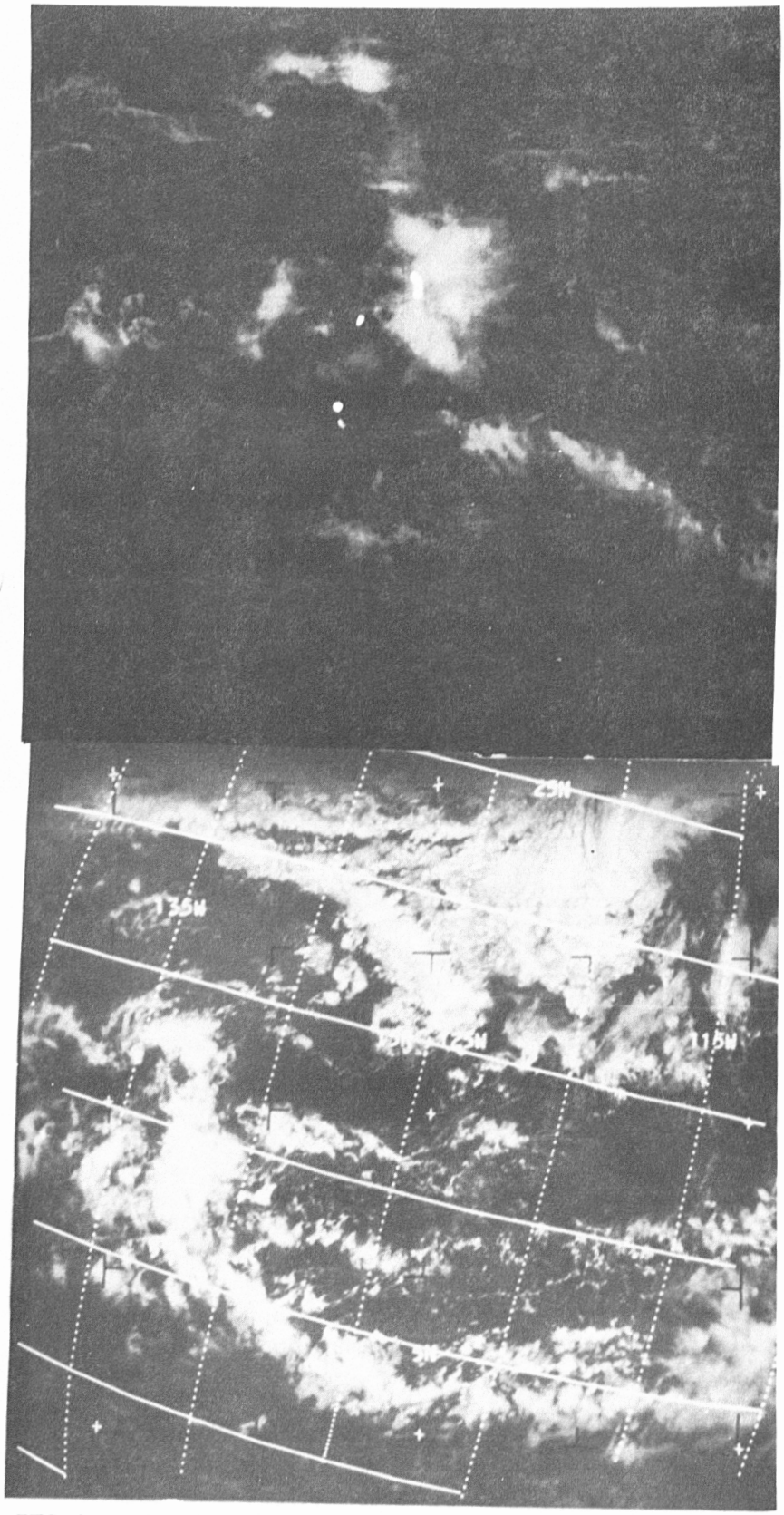

B.

Figure 14. ITC Area
A. ATS picture using full range table.
B. ESSA-5 frame.

A.

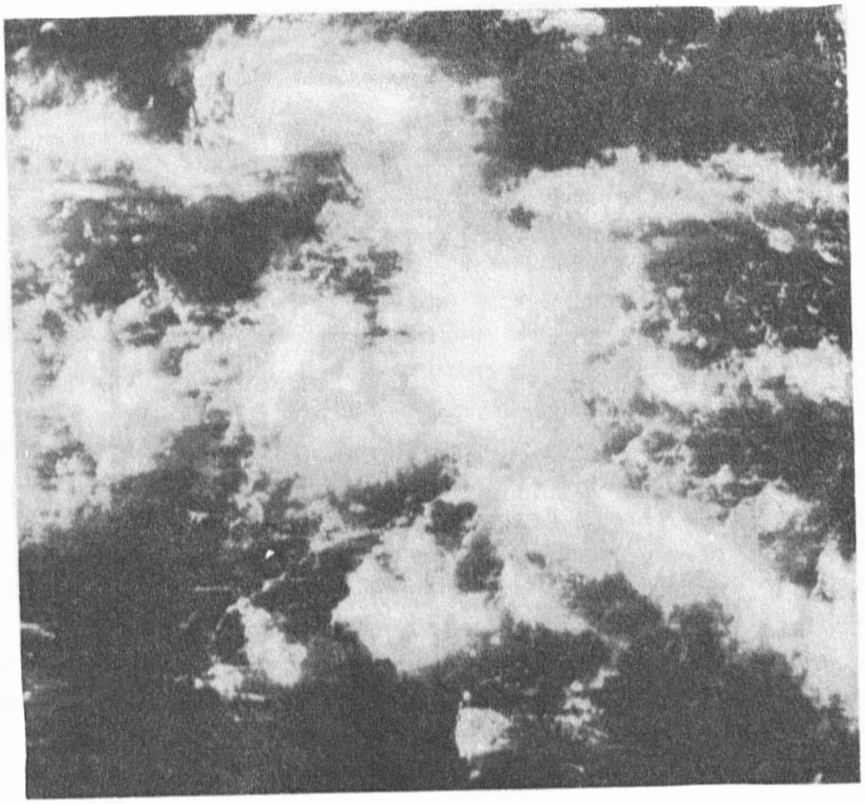

B.

Figure 15. ITC Area.
A. Low enhance table.
B. Portion of EIS frame, for same area.

A.

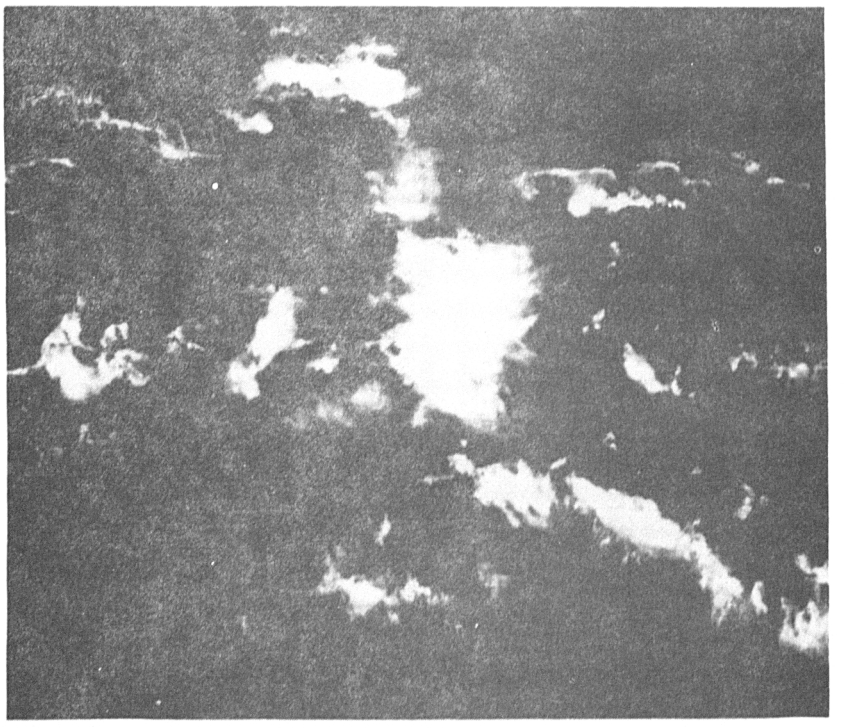

B.

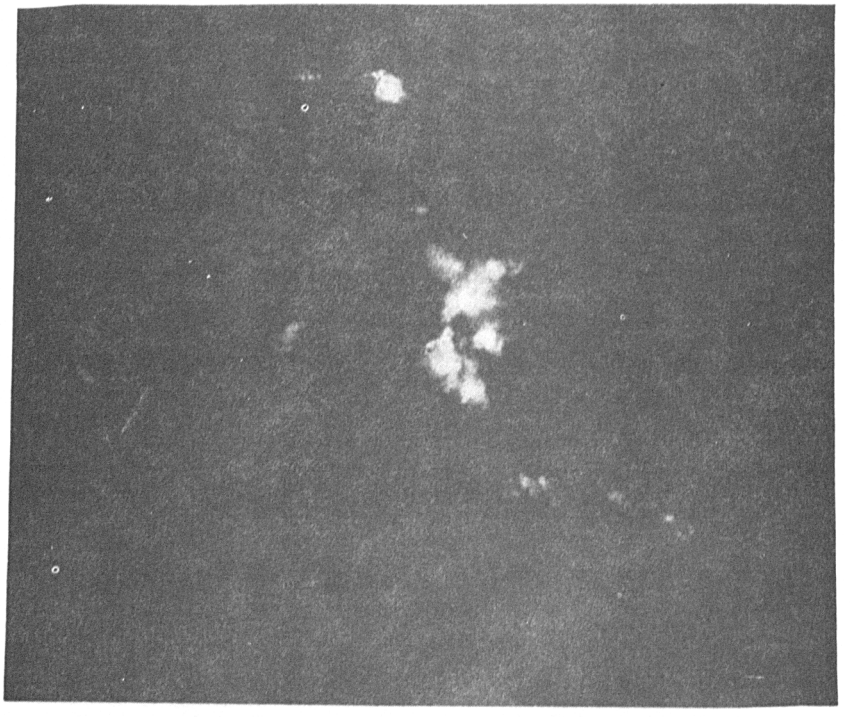

Figure 16. ITC Area.
A. Mid enhance table.
B. High enhance table.

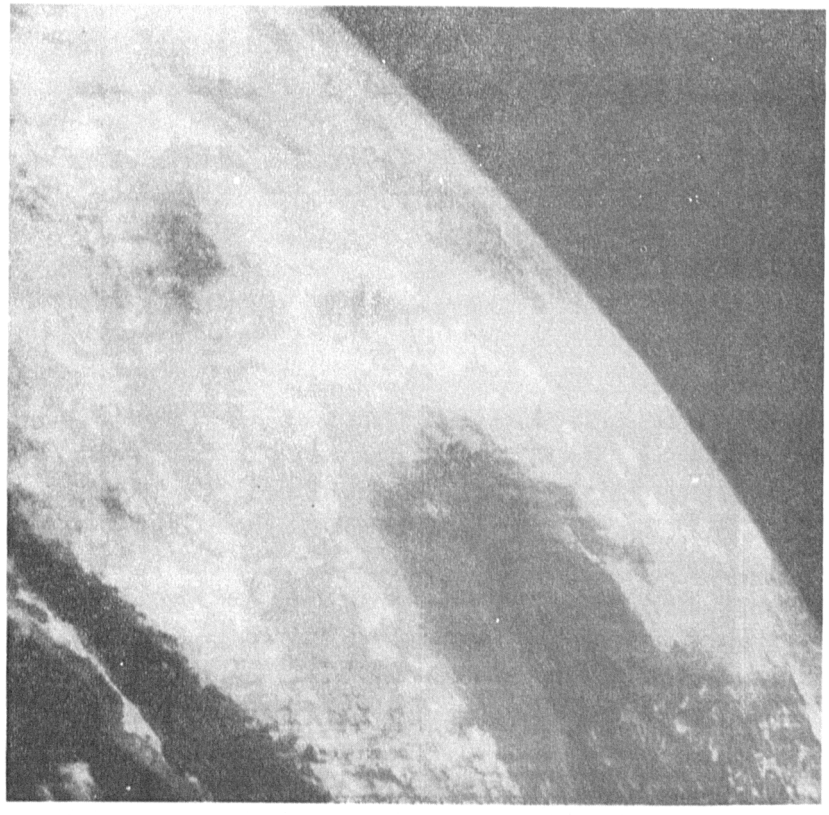

A.

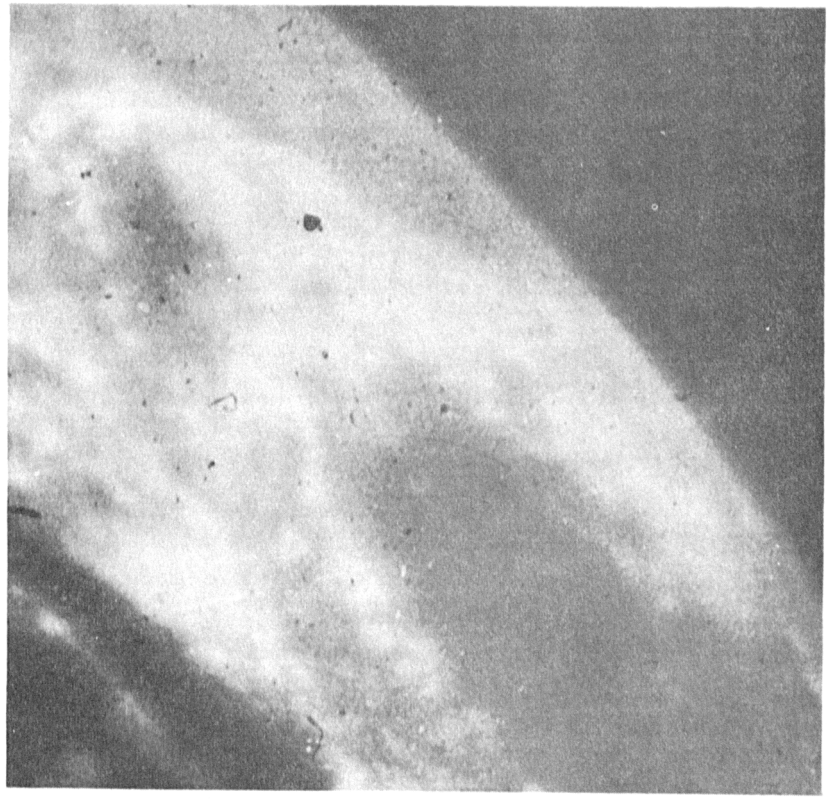

B.

Figure 17. Baja California Area.
A. Low enhance table.
B. Portion of EIS frame for same area.

A.

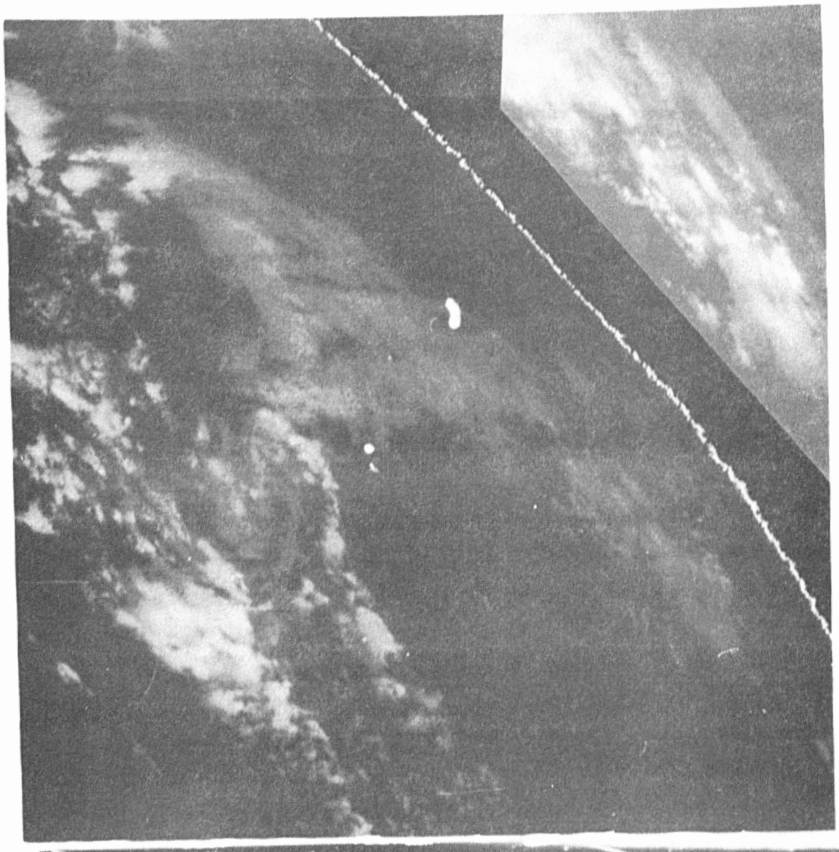

B.

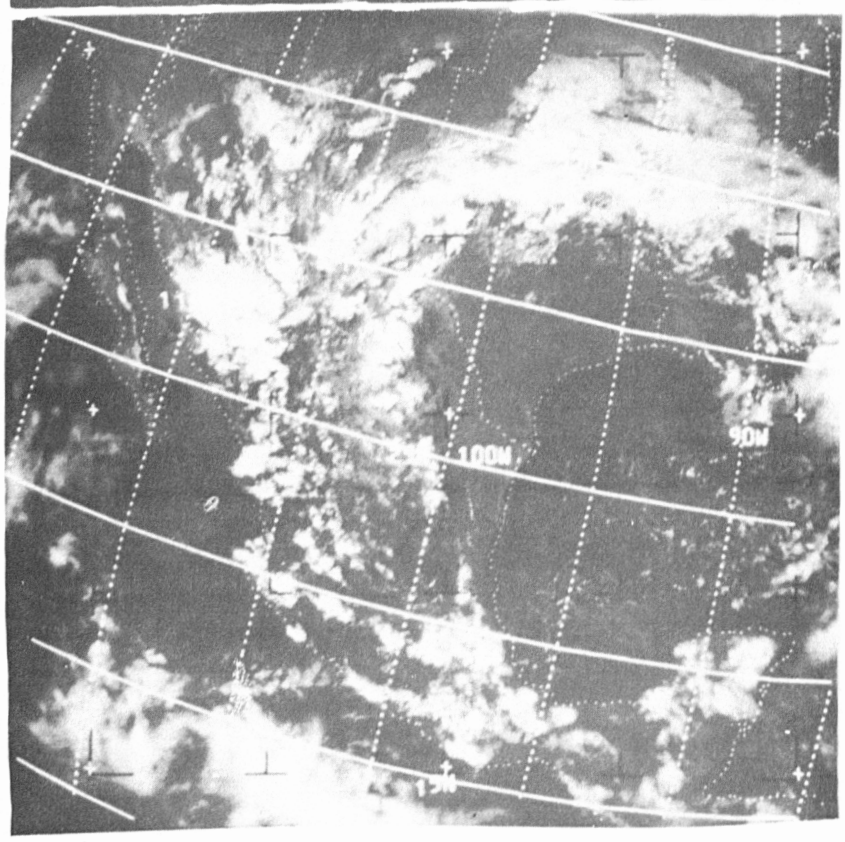

Figure 18. Baja California Area.
A. ATS picture using horizon table. Insert section using mid enhance table.
B. ESSA-5 frame.

The Hawaiian Islands area was chosen to test the LK2X2 program. This area is located just a little left of center in Figure 11. The very low range table was used in an attempt to enhance the geographical features. The result is shown in Figure 13 along with a Hawaiian map section enlarged to the same scale. The islands appear to be mostly cloud covered except for the peaks on the Island of Hawaii. Any attempt to increase the size of the sample matrix, i.e., 3X3, 4X4, would greatly increase the graininess and probably destroy eye appeal.

A cloud area on the Intertropical Convergence (ITC) just to the right of center in Figure 11 is depicted in Figures 14, 15 and 16. These displays are the output of the LK1024 program. The full range table was used in Figure 14a. It demonstrates the difficulty in applying a linear table as the less bright clouds are either missing or barely discernable. This difficulty will be compounded when calibrations, different gain settings, and sun angles are included in the computations. The ESSA-5 frame taken 1½ hour earlier is shown in Figure 14b. To try to bring out as much detail as possible and still retain some eye appeal, the low enhance table was used to produce Figure 15a. The same section from the EIS photo, again increased to the same scale, is shown in Figure 15b. Of interest is the thin cloud line in the lower right center which can be faintly seen on the ESSA-5 frame. The mid enhance table was used to produce Figure 16a. The protrusions of the central bright areas are more clearly defined. The three finger-like cloud structures are also clearly shown although the separation is better in the full range depiction. In Figure 16b. the disappearance of the left-most finger and the distinct separate bright areas of the central cloud mass are features brought out when the high enhance table is applied to the data.

Baja California, at approximately 6° azimuth, is a prominent landmark in the SSCC pictures. Views of it, the Gulf of Mexico, and the horizon, produced by LK1024, are shown in Figures 17 and 18. The low enhance table was used in Figure 17a. to bring out terrain features. The channel between Tiburon Island and the mainland is discernable. The EIS section, again to scale, is shown in Figure 17b. To help with attitude detection, the display of the horizon was thought to be useful. Figure 18a. was produced using the horizon table. The view of the same area from ESSA-5, 27 minutes earlier, is shown in Figure 18b. The insert is the portion over the Gulf of Mexico which was digitally enhanced using the mid enhance table and then further enhanced photographically.

VI. SUMMARY AND CONCLUSIONS

The SSCC experiment has given a far-reaching opportunity to work with a high volume of meteorologically meaningful digital data. The sensor response characteristics and dynamic range have opened new vistas for information processing and display. With the synchronous satellite

altitude and the approximate two mile resolution at the subsatellite point, there is good indication that even higher resolution is obtainable. A higher spin rate, with a change in the raster line ratcheting could give more lines of data so that the number of lines could approximate the number of information elements per line. This would give a square picture with approximately the same resolution in the north/south direction as is present in the east/west direction in the satellite pictures. Some of the diagnostic work mentioned in other sections of this report support the need for, and the practicality of, higher resolution data from this sensor. The proven dynamic range and the digitizing to a 256 count have permitted meaningful tests on which different information can be emphasized by a variety of treatments. In this category, enhancement to show terrain, thunderstorm cells, and cirrus plumes can be realized with a variety of digital techniques.

Suggestions for future experiments: The following suggestions are given with the thought that some of them may represent changes already made or planned for future ATS satellites.

A. Spacecraft

1. Some change of hardware may be required to minimize problems of momentum balance which appear to impart a nutation to the satellite. In the studies of horizon detection in Section 4, the center line of pictures appears to follow a complex curve from the top to the bottom data line. This may well be from the use of a feedback circuit in the present analogue sun pulse circuitry or from the mechanical notation mentioned above.

2. Some more accurate method of obtaining line-to-line synchronization needs to be worked out. This might be from horizon sensors or the stepping of lines from an inertial coordinate base. For future ATS satellites it is highly desirable that star mappers be included to supply data for attitude determination. This could make possible the determination of attitude as often as once a minute with accuracy superior to that from the horizon images from a smaller volume of data. With attitude known as a function of time before the picture data is processed, undistorted horizon sample numbers could be computed for pictures with only one horizon illuminated, and the difference between computed and observed horizon positions could be used for differential line-by-line shifting to provide better picture coherence. This in turn should make possible greater accuracy in gridding pictures and mapping brightness distribution.

B. Digitizing Ground Facility

1. Digital tape must be carefully formatted and written so that it may be processed thru as wide a variety of computers as possible. Numerous problems have arisen with the combination of computer, magnetic tape, and ground station resources employed in the present experiment.

2. Noise suppression and diagnostic correction procedures should be done at the data acquisition site. This correction could include a continuous study of the digital range of the recorded data. A regular check should be made on the frequency distribution of the digital data. Such a facility suggests the use of a small computer in the initial tape writing and certification procedures.

3. Picture digitizing facilities should be augmented and upgraded to provide complete recording of each frame and thus obviate the need for the current procedure of digitally recording every other frame.

C. Data Communication and Processing

The increasing data volume and proliferation of sensors indicates a need for a highly specialized, dedicated computer facility.

Some transmission facility such as a wide band link or satellite relay will be needed to get pictorial or descriptor information from the computer facility to the users.

D. Display Needs

The increase of data volume and the increased dynamic range of the sensor makes more acute the need for improvements in the display facilities. A display matrix of at least 8000 by 8000 will soon be required. The present dynamic display range is limited to between twelve and fifteen steps and this should be increased. One method by which the number of discernable shades could be augmented is by the use of color tones, where various density steps could be used in one color and then repeated in one or more other colors.

As a larger matrix is attained for display it becomes obvious that an increase of input-output rate from the computer to the display device is required. Higher density magnetic tapes and higher tape speeds may be stop gap measures but soon there must be a system which does not use magnetic tape as a buffer to the display. This will effect several efficiencies and will permit high volume displays to be produced in a shorter time. If the magnetic tape can be eliminated from this process, the output rate can more closely approach the potential of a modern digital computer.

ACKNOWLEDGMENTS

We wish to thank Mr. C. L. Bristor of the Data Processing & Analysis Division of NESC for helpful comments and suggestions. We wish also to thank Dr. S. Fritz of the Meteorological Satellite Laboratory (MSL) for important discussions in connection with scale of cloud systems, and Mr. L. F. Hubert, MSL for discussions on the geometry of the spin scan cloud camera.

Our thanks also to Messrs. R. E. Bradford and A. Booth for work on spectral analysis, Levin Lauritson for extensive work with sun terminator lines on the geographic picture grids, and Marcus Shellman for his programs which merge grid information with picture brightness for input to the digitally driven display devices.

REFERENCES

1. Bristor, C. L., 1966, "Satellite Data Collection", Proceedings of the IBM Scientific Computing Symposium on Environmental Sciences, Thomas J. Watson Research Center, Yorktown Heights, New York, pp. 5-17.

2. Bristor, C. L. and W. M. Callicott and R. E. Bradford, 1966. "Operational Processing of Satellite Cloud Pictures by Computer", Monthly Weather Review, Volume 94, Number 8, pp. 515-527.

3. Doolittle, Russell C., 1963, "Calibration of Image Distortion in TIROS Wide Angle Photography", U. S. Weather Bureau, Meteorological Satellite Laboratory, Report Number 15.

4. Frankel, M. H. and C. L. Bristor, 1962, "Perspective Locator Grids for TIROS Pictures", U. S. Weather Bureau, Meteorological Satellite Laboratory, Report Number 11.

APPENDIX 1

Format of NESC Generated Input Data Tape

The raw data digital tapes, produced at the ground stations were received at NESC in irregular intervals. All tapes were logged in and selection of those to be copied was made to provide inputs for the various experiments being conducted at NESC. Because of CDC 6600 computer limitations, the tapes cannot be read on the standard higher speed CDC 607 tape drives. The tapes are therefore read on a slower speed tape unit, the CDC 604, which is available to the computer system via a remote cable. A special software routine is required to read the tapes with their high density and "long" record lengths. The copy-and-edit (CE) program, using the above routine, reads the tape, removes certain non-information bits or indicates their absence, reformats the documentations, crops off a fixed arbitrary number on "space" samples from the extremities of each line and writes a logical record consisting of two 512-(60-bit) word physical records at 800 bpi for each line (record) on input. The format of the output tape is given below. The end of the image is indicated by an end of file.

Word 1 - OPPPPPPPPPPPPFFFFFFFFFFFFOOODSMOOOGGGLLLLLLLLLLLLLLLLLLLLLL

Word 2 - OOOOOOTTTTTTTTTTTTTTTTTTTTTTTTTTTTTTTTTTTTTTTTTTTTTTTTTTTTTT

Words 3 to 1024 - Packed 8-bit data samples.

P - Phase-locked loop error (Binary)
F - Frame ID (BCD)
D - Scan direction(S to N "1", N to S "0")
M - Scan mode (Normal "1", back to back "0")
S - Satellite gain (High "1", Normal "0")
G - Ground gain (BCD)
L - Line count (BCD)
T - Time, GMT time, days, hours, minutes, seconds (BCD)

Those indicated to be BCD are not normal BCD in that zero (0) is 00 instead of 12. This program has undergone several revisions as problems came up and were overcome. The average central processing (CP) time is 2.6 minutes per tape. The program produces a core dump of the last two records processed which is another diagnostic tool. Success in reading the raw data tapes has varied and considerable effort has been expended in evaluating tape quality, optimizing both the special input routine and tape handling procedures on the 6600, and checking the ground station digital equipment. Hopefully the problems encountered show the areas where improvements are needed in future experiments and in eventual operational systems.

APPENDIX 2

United Aircraft Facsimile Encoder

The encoder is an electronic converter which reads information from a digital magnetic tape and changes the information to electrical signals. These signals are fed to a standard weather facsimile recorder which displays in sepia on a specially treated moistened paper roll. The encoder can be operated at speeds of 120, 480, or 960 lines per minute and may be used in either a "black and white" mode or in a gray scale mode where there is a choice of gray shades. Information for display is read from a magnetic tape written at 556 bpi density. A CDC Model 603 tape drive is employed.

The encoder has a 2048-byte memory but a line of data in either black and white (single-bit), or in the gray scale mode (3 bit) mode is limited to 1710 bytes per facsimile scan line. The length of a display in terms of scan lines (at 96 lines per inch) is limited to the volume of data which can be stored on a single magnetic tape. More than 14 feet of imagery can thus be displayed as a unit in cases where the black and white mode is used.

Each line of output thru the encoder is from a separate tape record and an end of file stops the device, which starts up on another output frame unless a second tape end of file is found in which case the device is shut off.

The resolution of the device, in either mode is 96 bytes per inch and also 96 lines per inch for a square picture element. Due to the fact that the display is from a helical burning wire the device has some smearing along a line. Some care must be taken in the use of the Fax Encoder to be sure that the display paper is uniformly moist or picture characterisitcs will be below standards.

This encoder is also used for data transmission over a normal facsimile quality line. When used for transmission it is operated at 120 lines per minute.

Link Division Weather Satellite Digital and Analogue Display

This display device operates either from a direct analogue signal source or from computer produced digital information. The digital information is fed from a CDC 603 tape drive with the data recorded at 556 bpi.

There are three main modes in which this cathode ray tube display device is used:

Analogue data display
Digital data display
Analogue and digital data displayed on the same film.

When used as a digital display device the CRT can be addressed as a 1024 by 1024 matrix or alternately as a 2048 by 2048 matrix. Choice of the digital mode is made by a console switch. Digital data may be input in four bit bytes or six bit bytes. Choice of the byte size is under programmer control.

The CRT plot shows on a 1.38 by 1.38 inch square which is recorded on 35-mm films as a 0.92 by 0.92 inch square area. Optional polaroid prints can be made with or without 35-mm film on any picture.

The link device can be used to draw solid, dashed, or broken lines in various line weights or it may be used to produce a digital picture by input of data a line at a time. The device works with a flying spot scanner where the input data modulates the intensity of light of the flying spot.

A character set is available so that alphanumeric characters may be displayed either with analogue or with digital data information. These characters which include some special meteorological symbols can be output in a number of sizes and weights under program control.

APPENDIX 3

Horizon Data Input for Attitude Determination: Computer Search Logic and Output Tape Format

Input to the horizon search program ATSRD was on high density (800 bpi tapes), one per picture, with data reformatted and the number of samples per line reduced to 7165 by cropping 256 samples (normally space view) from each end. These tapes were provided by the copy-and-edit program described above. Several revisions of the search logic were required before horizon detection was adequate. Initially, search was started at the extremities of each line of data outside the horizon and proceded toward the center until 2 successive samples with brightness value greater than 1 were encountered. This proved ineffective because of noise in the space viewed samples. The logic was then changed to start from near the center and work outward until two successive samples with less than 6 were found. This higher threshold proved satisfactory for a fully illuminated earth disk, with little loss of accuracy because of the rapid drop off of brightness at the earth-space interface. However, still further revision was necessary for early morning or late afternoon pictures in which only a small crescent of earth is illuminated near the sunlit horizon. The final procedure involves a start at the center of the picture and search outward until 4 successive samples with brightness greater than 5 are reached. At this point a flag is set and the search continued until 4 successive samples of brightness less than 6 are found. At this point the current sample number (adjusted for the successive space samples used) was stored in the output buffer and search proceeded to the next line. In the event that no horizon point was found before the end of the line, pre-stored zeros were left unchanged in the output buffer.

The output tape contains one file of two records. The first record contains 10 words: day of year count, picture start time hours, minutes, and seconds, and a count of the number of lines processed for this picture. (The last five words are dummy words to reserve space in the format for possible future use.)

The second record consists of 2017 x 8 words giving for each line processed: (1) the line sequence in the processing program (not necessarily the position in the picture), (2) the left horizon sample number, (3) the right horizon sample number. Words (4) and (5) are zeros to reserve space for adjusted horizon sample numbers corrected for the drift of the mid-horizon position from line to line, if such correction becomes feasible. The remaining words are obtained from the documentation for each line of the digital tape received from the ground station:(6) time (minutes), (7) time (seconds), (8) the sequence number of the line in the picture.

APPENDIX 4

Input Information for Attitude Determination Program.

The following information is input to the attitude determination program on punched cards:

(a) Picture identification for printout.
(b) Satellite number, ground station identifier, pass number, picture mode (taped or direct), and camera number, all to be punched on cards by the computer for input to the LINK (CRT) gridding program.
(c) Logical unit number for input tape and codes to select desired optional diagnostic printout.
(d) Epoch date/time (year, month, day, hour, minute, second GCT) and corresponding orbital elements (right ascension of ascending node, rate of change of ascending node right ascension in degrees per day, inclination, period) and Greenwich Hour Angle of Aries at epoch time.
(e) The number of pictures to be processed.
(f) The maximum number of samples per line and lines per picture, and the line and sample number for the midearth position of the telescope when it is normal to the spin axis.
(g) Angular changes in telescope position from one line to the next (radians per line) and from one sample to the next along a line (radians per sample).
(h) Field of view angles — maximum angular displacement of the telescope from its mid-position corresponding to the end samples of a line (rotation about the spin axis) and to the top and bottom lines (displacement from the spin axis perpendicular). (These angles are used with the maximum line and sample numbers to generate the angular change per spot and line when the information fields listed under (g) above are left blank.)

(i) Constant coefficients s1, s2 for the linear equation used to approximate the shift in midearth sample number across the picture.

$$I_0 = I_{MID} + s1 + s2\,(J - J_0)$$

where I_{MID} = central sample number of data for line (3833)

J = line number of point on picture horizon

J_0 = line number for which telescope is normal to spin axis

(j) Option codes to select alternate computational methods or outputs.

(k) For each picture: date (year, month, day), start time (GCT: hours, minutes, seconds), subsatellite point latitude and longitude, height of the satellite, line and sample numbers for the mid-position of the telescope, and number of lines for this picture. Because of time constraints* in real time processing of the data at the ground station the number of lines per picture varied greatly and almost always was less than the nominal 2000 lines, sometimes less than 1200. Rather than change the line sequence numbers (input with the horizon sample numbers) to correspond to their position in a complete picture, separate line/spot numbers were input for each (partial) picture to designate the mid-point of the complete picture.

APPENDIX 5

<u>Procedure for Computing the Angular Increment Between Successive Samples On A Line, From A Picture With Two Horizons</u>

1. Convert the satellite location to geocentric cartesian coordinates with X axis in the vernal equinox, Y axis at 90° right ascension and Z axis along the north polar axis of the earth, (Xs, Ys, Zs).

2. Compute 9 elements of the orientation matrix relating the camera axes to the axes of the coordinate system in step 1.

   Camera X axis: horizontal, perpendicular to spin axis, positive to right (east).

---

* Additional tape drives are required so that one can be on standby to await the arrival of the next picture while the tape for the current picture is being rewound and unloaded.

Camera Y axis: parallel to spin axis, positive toward northern hemisphere.

Camera Z axis: to make right handed orthogonal system.

The orientation matrix can be generated by 4 rotations which take the camera axes into the celestial coordinate system of step 1.

(1) Clockwise about camera X axis by the picture tilt to bring the Y axis to horizontal.
(2) Counter clockwise about the new Z axis by the principal plane azimuth to bring the Y axis (spin-axis) into north.
(3) Clockwise about the new X axis (east) by the satellite co-latitude to bring the Y axis into the equatorial plane with right ascension equal to that of the satellite plus 180 degrees.
(4) Clockwise about the new Z axis (north polar) by 90 degrees plus the right ascension of the satellite to bring the Y axis to 90 degrees right ascension and the X axis into the vernal equinox.

3. For each picture line containing both horizons, compute the mid-earth sample number, and the number of samples from mid-earth to the right horizon (ΔI).

4. Compute camera coordinate angles for the perspective ray to the right horizon point.

$$\alpha = (J_0 - J) \quad *.000131$$

$$\beta_0 = \Delta I \quad *.00004261$$

Jo is the line number of the picture center and J of the horizon point. β_0 is an initial approximation for β , to be improved by iteration.

5. Compute camera coordinate system directior cosines for the perspective ray to the horizon point.

$$l = \cos\alpha \sin\beta$$

$$m = \sin\alpha \qquad \text{(on first iteration } \beta = \beta_0\text{)}$$

$$n = \cos\alpha \cos\beta$$

6. Multiply the direction cosines from step 5 by the orientation matrix from step 2 to obtain the direction cosines of the perspective ray to the horizon point in the celestial coordinate system of step 1. (L, M, N)

7. Form the coefficients of the quadratic equation for the slant range along the horizon point perspective ray from the satellite to its intersection with the earth by substituting

for $X = LS + X_s$

$Y = MS + Y_s$

$Z = NS + Z_s$

into the equation for the earth ellipsoid:

$$\frac{X^2}{a^2} + \frac{Y^2}{a^2} + \frac{Z^2}{a^2(1-e^2)} = 1$$

where: L, M, N are the direction cosines from step 6,
Xs, Ys, Zs are the satellite coordinates from step 1,
X, Y, Z are the coordinates of the point of intersection of the perspective ray with the ellipsoid,
S is the slant range, satellite to earth intersection,
a is the equatorial radius of the earth,
e is the eccentricity of the meridional ellipse.

The resulting equation is:

$$AS^2 + BS + C = 0$$

where:

$$A = 1 - e^2(L^2 + M^2)$$
$$B = 2(1-e^2)(LX_s + MY_s) + 2NZ_s$$
$$C = R_s^2 - e^2(X_s^2 + Y_s^2) - (1-e^2)a^2$$

where R_s is the geocentric radius to the satellite.

8. Test the sign of the quantity (B^2 - 4AC) in the radical for the standard solution to the equation in step 7. (If positive there are two solutions and the ray intersects the earth. If negative there is no solution and the ray misses the earth.)

a) For a positive value set a flag to indicate intersection, increase β by $\Delta\beta$ (initially the angular increment is set as a convenient value, e.g. 0.02 radians), and return to step 4. When the radical becomes negative, set a flag to indicate no intersection and decrease β by $\Delta\beta/2$. Once both flags are set

the adjustment $\Delta\beta$ is halved at each trial and is added following a positive value of $\beta^2 - 4AC$ and subtracted following a negative value of $\beta^2 - 4AC$. Iteration is stopped when $\Delta\beta$ is less than some arbitrary value, e.g. 0.000001 radian.

b) For a negative value of $\beta^2 - 4AC$ on the first iteration, β is decreased by $\Delta\beta$ until earth intersection is indicated and thereafter adjustment of β is as under a) above.

9. For each line compute the angular increment between samples from $\beta/\Delta I$ where β is the final value determined in step 8 and ΔI is the number of samples from midearth to the horizon point, computed in step 3.

10. Average the values for each line to find a mean value and standard deviation.

11. Subtract the mean value from that for each line to form residuals. Reject values with residuals larger than three times the standard deviation.

12. Recompute the mean value and standard deviation.

APPENDIX 6

Computation of Image Nadir Point Sample and Line Numbers

The sample and line number of the picture nadir points were computed using a least-squares solution to the observational equation set:

$$\cos\alpha_i \sin\beta_i \, \ell_N + \sin\alpha_i \, m_N - \cos\alpha_i \cos\beta_i \, n_N = \cos\theta_i \quad [3]$$

where ℓ_N, m_N, n_N are direction cosines of the perspective ray to the nadir point (to be solved for).

α_i, β_i are coordinate angles for perspective rays to horizon images as previously defined.

The functions of α_i and β_i forming the coefficients of the left hand members are direction cosines of the perspective rays to the horizon points.

The nadir spot/line coordinates were then computed from:

$$I_N = I_o + \arctan(\ell_N / -n_N) \,/\, 0.00004261$$

$$J_N = J_o - \arctan\left(m_N / \sqrt{\ell_N^2 + n_N^2}\right) / 0.000131$$

where I_o, J_o are the sample number and line assigned to the picture center. (Different choice of picture center coordinates I_o, J_o would result in different values for α and β, for the coefficients in equation [3], and for the direction cosines ℓ_N, m_N, and n_N.) The resulting differences in the arc tangents would offset the changes in I_o, J_o and the values obtained for I_N, J_N would stay unchanged. In other words, the position of the nadir point (where the center of the earth disk is imaged) is fixed relative to the sample/line coordinate system used for the picture data.

APPENDIX 7

Iterative Procedure for Finding Picture Center From Horizon Sample/Line Numbers

The residuals formed in the least-squares solution of system [1],

$$v_i = \cos\alpha_i \cos\beta_i \cos\phi - \sin\alpha_i \sin\phi - \cos\theta_i$$

are implicitely dependent on the values used for I_o, J_o

$$\alpha_i = (J_o - J_i) * 0.000131$$

$$\beta_i = (I_i - I_o) * 0.00004261$$

$$\phi = (J_N - J_o) * 0.000131$$

where J is the line number of the image nadir point. In the case of ideal perfect data, the residuals v_i would all be zero.

$$F = \cos\alpha_i \cos\beta_i \cos\phi - \sin\alpha_i \sin\phi - \cos\theta = 0$$

expressing F by the linear terms of the Taylor series and dropping subscripts

$$F = F_o + \frac{\partial F}{\partial \alpha}\frac{\partial \alpha}{\partial J_o}\Delta J_o + \frac{\partial F}{\partial \alpha}\frac{\partial \alpha}{\partial I_o}\Delta I_o$$

$$+ \frac{\partial F}{\partial \beta}\frac{\partial \beta}{\partial J_o}\Delta J_o + \frac{\partial F}{\partial \beta}\frac{\partial \beta}{\partial I_o}\Delta I_o$$

$$+ \frac{\partial F}{\partial \phi}\frac{\partial \phi}{\partial J_o}\Delta J_o + \frac{\partial F}{\partial \phi}\frac{\partial \phi}{\partial I_o} I_o$$

provides a set of linear equations which may be solved for adjustments (ΔI_o, ΔJ_o) to the picture center.

$$\frac{\partial F}{\partial \alpha} = -\sin\alpha\cos\beta\cos\phi - \cos\alpha\sin\phi$$

$$\frac{\partial F}{\partial \beta} = -\cos\alpha\sin\beta\cos\phi$$

$$\frac{\partial F}{\partial \phi} = -\cos\alpha\cos\beta\sin\phi - \sin\alpha\cos\phi$$

$$\frac{\partial \alpha}{\partial J_o} = 0.000131 \qquad \frac{\partial \alpha}{\partial I_o} = 0$$

$$\frac{\partial \beta}{\partial J_o} = 0 \qquad \frac{\partial \beta}{\partial I_o} = -0.00004261$$

$$\frac{\partial \phi}{\partial J_o} = -0.000131 \qquad \frac{\partial \phi}{\partial I_o} = 0$$

With substitution of the above partial derivatives the equations reduce to the form

$$(A_1 + A_2)\Delta J_o + B\Delta I_o = F - F_o \qquad [4]$$

where $A_1 = (-\sin\alpha\cos\beta\cos\phi - \cos\alpha\sin\phi) * 0.000131$

$A_2 = (-\cos\alpha\cos\beta\sin\phi - \sin\alpha\cos\phi) * (-0.000131)$

$B = (-\cos\alpha\sin\beta\cos\phi) * (-0.00004261)$

$F = 0$

F_o = The set of residuals from the initial solution for $\sin\phi$ and $\cos\phi$

New values for the picture center coordinates are formed using the least-squares solution of the equation set [4].

$$I_o = I_o + \Delta I_o$$

$$J_o = J_o + \Delta J_o$$

These values are then used to find new values for α, β and the solution for $\sin\phi$, $\cos\phi$ is repeated forming a new set of residuals. Since only the linear terms of the Taylors series are used, iteration must be continued until the error from neglecting the higher order terms becomes insignificant.

APPENDIX 8

Image Geometry of Conventional and Spin Scan Cameras

The procedure used in the gridding program to compute image coordinates for rays from ground points at selected latitudes and longitudes is described elsewhere (Frankel, 1962). There are 4 basic steps in the procedure.

1. Azimuth and nadir angles at the satellite are computed for an incident ray from the latitude/longitude of the point and the latitude, longitude, and height of the satellite.

2. Coordinates ($\tan \Delta\alpha$, $\tan \Delta\beta$) are computed in a positive image plane at unit distance from the perspective center, making use of the azimuth and nadir angles of the optical axis of the camera. $\Delta\alpha$, $\Delta\beta$ are orthogonal direction angles measured from the optical axis $\Delta\alpha$ in the principal plane, positive toward the horizon.

3. Rectangular image coordinates for unit focal length are computed as follows:

$$\Delta x = \tan u \cos(\gamma - \delta)$$

$$\Delta y = \tan u \sin(\gamma - \delta)$$

where Δx, Δy are image plane displacements from the principal point, and the x axis is parallel to the top and bottom edges of the picture format, positive to the right.

$$\tan u = \sqrt{\tan^2 \Delta\alpha + \tan^2 \Delta\beta}$$

$$\tan \gamma = \tan \Delta\alpha / \tan \Delta\beta$$

and δ is the clockwise rotation in the image plane from the positive y - axis to the upper end of the principal line.

4. If symmetrical radial distortion is to be applied the coordinates are modified to:

$$\Delta x' = \tan \phi \cos(\gamma - \delta)$$

$$\Delta y' = \tan \phi \sin(\gamma - \delta)$$

where $\tan \phi = \tan u\,(1 - k_1 u - k_2 u^2)$ where k_1 and k_2 are constants determined in a prelaunch distortion calibration program (Doolittle, 1963).

These coordinates (which have been computed for unit focal length and origin at the picture center) require further modification when the grid points are to be merged with a digital display whose coordinates are expressed in terms of line number J and sample number I.

$$I = I_{pp} + C \cdot \Delta x'$$

$$J = J_{pp} - C \cdot \Delta y'$$

where I_{pp} , J_{pp} are spot and line coordinates of the picture center and C is the focal length of the camera in "raster units" (I_{pp} , J_{pp}, and C are computed in the prelaunch distortion calibration from target control points whose image coordinates are input as line and spot numbers).

For gridding the ATS1 pictures, the standard program logic was used to compute the unit focal length image coordinates Δx, Δy as in step 3 above. The input aximuth and nadir angles for the optical axis, required in step 2, were computed in the attitude determination program. The spin axis vector was resolved into north, east, and up components, and aximuth and instantaneous roll angles were computed from them. The optical axis nadir angle was set equal to the magnitude of the spin axis roll. For positive roll angles the azimuth of the principal plane was that of the vertical plane containing the spin axis, and the swing angle " δ " in step 3 was made 0°. For negative spin axis roll angles, the principal plane azimuth was changed by 180° and δ was made 180°.

An alternate logic loop was inserted in the subroutine which converts image coordinates to sample/line numbers in the digitized picture. For the conventional camera, the unit focal length coordinates Δx, Δy, -1 may be regarded as direction numbers of a perspective ray of length $\sqrt{1 + \Delta x^2 + \Delta y^2} = \sqrt{1 + \tan^2 u}$. The corresponding direction cosines are $\Delta x \cos u$, $\Delta y \cos u$, and $- \cos u$. For a perspective ray in a spin scan picture the direction cosines are $\cos\alpha \sin\beta$, $\sin\alpha$, and $- \cos\alpha \cos\beta$ where α is the cant angles of the telescope from the spin axis normal, and β is the spin displacement from the mid-earth position.

By equating corresponding direction cosines,

$$\tan\beta = \frac{\ell}{-n} = \Delta x$$

$$\tan\alpha = m / \sqrt{\ell^2 + n^2} = \Delta y \cos\beta$$

Finally, the digital coordinates are computed as

$$I = I_o + \beta / .00004261$$

$$J = J_o - \alpha / .000131$$

where I_o , J_o are the sample/line numbers of the picture center.

If, in future experiments, the shift in mid-earth spot number can be determined as a function of line number, it could be incorporated as a distortion term in the expression for I. However, it would be preferable to apply the shift as a correction to the sample numbers assigned to the brightness values on each line.

*26. Meteorological Products from Digitized Satellite Vidicon Cloud Pictures, C. L. Bristor and W. M. Callicott, (March 1964) AD 600078

27. A Summary of Experiences in Computer Processing of Nimbus I Data, C. L. Bristor, (June 1966)

28. Automatic Processing of Nimbus Infrared Radiometer Data, G. E. Martin and L. Rubin, (July 1964) PB 166590

*29. Tropospheric Conditions over the Tropical Atlantic as Observed by Two TIROS Satellites and Research Aircraft During 22 September 1962, H. M. Johnson and R. W. Fett, PB 167178

30. Lowlight Coverage from Polar and Sun-Synchronous Orbits, R. L. Pyle, (April 1964) AD 600970

*31. Specular Spectral Reflectance of Paints from 0.4 to 40.0 Microns, W. Y. Ramsey, (April 1964) PB 167179

*32. TIROS Photographs and Mosaic Sequences of Tropical Cyclones in the Western Pacific During 1962, R. W. Fett, (July 1964) AD 608095

*33. Wind Speeds from TIROS Pictures of Storms in the Tropics, A. Timchalk, L. F. Hubert, and S. Fritz, (February 1965) PB 167180

34. An Investigation of Degradation Errors in TIROS IV Scanning Radiometer Data and the Determination of Correction Factors, P. K. Rao, E. G. Astling, and F. J. Winninghoff, (October 1965)

35. Project Storm Cloud - An Aircraft Satellite Case Study of an East Coast Cyclone. Part I - Descriptive Aspects, E. Paul McClain and L. F. Whitney, Jr., (December 1965)

36. Experimental Use of Satellite Pictures in Numerical Prediction, Part II, H. J. Brodrick, E. P. McClain and M. A. Ruzecki, (January 1966)

37. Mesoscale Cellular Convection, L. F. Hubert, (May 1966)

38. Angular Distribution of Solar Radiation Reflected from Clouds as Determined from TIROS IV Radiometer, I. Ruff, R. Koffler, S. Fritz, J. S. Winston, and P. K. Rao, (December 1966)

39. Motions in the Upper Troposphere as Revealed by Satellite Observed Cirrus Formations, H. McClure Johnson, (December 1966)

40. Cloud Measurements Using Aircraft Time-Lapse Photography, L. F. Whitney, Jr., and E. Paul McClain, (April 1967)

41. The SINAP Problem: Present Status and Future Prospects. Proceedings of a Conference held at the National Environmental Satellite Center, Suitland, Maryland, January 18-20, 1967, E. Paul McClain, (October 1967) PB 176570

42. Operational Processing of Low Resolution Infrared (LRIR) Data from ESSA Satellites, Louis Rubin, (February 1968)

43. Atlas of World Maps of Long-Wave Radiation and Albedo -- For Seasons and Months Based on Measurements from TIROS IV and TIROS VII, J. S. Winston and V. Ray Taylor, (September 1967) PB 176569